NASA CONTRACTOR REPORT

COMBUSTION PROCESS OF IMPINGING HYPERGOLIC PROPELLANTS

by L. B. Zung and J. R. White

Prepared by
MARSHALL INDUSTRIES
Irvine, Calif. 92664
for Lewis Research Center

NATIONAL AERONAUTICS AND SPACE ADMINISTRATION • WASHINGTON, D. C. • MAY 1971

1. Report No.	2. Government Accession No.	3. Recipient's Catalog No.
NASA CR-1704		

4. Title and Subtitle	5. Report Date
COMBUSTION PROCESS OF IMPINGING HYPERGOLIC PROPELLANTS	May 1971
	6. Performing Organization Code

7. Author(s)	8. Performing Organization Report No.
L. B. Zung and J. R. White	SN-145-F
	10. Work Unit No.

9. Performing Organization Name and Address	11. Contract or Grant No.
Marshall Industries 2400 Michelson Drive Irvine, California 92664	NAS 3-12031
	13. Type of Report and Period Covered
12. Sponsoring Agency Name and Address	Contractor Report
National Aeronautics and Space Administration Washington, D.C. 20546	14. Sponsoring Agency Code

15. Supplementary Notes

Film supplement C-273 available on request.

16. Abstract

Single exposure photography and high speed motion pictures were used to study the sprays formed by impinging streams of liquid hydrazine and nitrogen tetroxide. Chamber pressures were varied between 15 Psia and 500 Psia. Four different orifices (.027" to .060") were used. Propellant temperatures and velocities were varied from 40^{o} F to 140^{o} F and 15 ft/sec to 95 ft/sec, respectively. Influence of chamber pressure and propellant temperature on separation and mixing were determined. Effects of orifice diameter and chamber pressure on the occurrence of popping were quantitatively evaluated.

17. Key Words (Suggested by Author(s))	18. Distribution Statement
Stream separation Combustion popping Liquid mixing	Unclassified - unlimited

19. Security Classif. (of this report)	20. Security Classif. (of this page)	21. No. of Pages	22. Price*
Unclassified	Unclassified	43	$3.00

*For sale by the National Technical Information Service, Springfield, Virginia 22151

FOREWORD

The research described in this report was conducted by the Dynamics Science Division of Marshall Industries under NASA contract NAS 3-12031. Mr. Richard J. Priem of the Lewis Research Center Chemical Rocket Division was the NASA Project Manager. The report was originally issued as Dynamic Science report SN-145-F.

TABLE OF CONTENTS

	Page No.
INTRODUCTION	2
EXPERIMENTAL APPARATUS	3
Combustion Chamber	3
Propellant Feed System	3
Recording Instrumentation	7
Photography	7
IMPINGEMENT EXPERIMENTS UNDER ATMOSPHERIC PRESSURE	9
Comparison with Previous Experimental Studies	15
STREAM MIXING/SEPARATION RESULTS WITH VARIOUS CHAMBER PRESSURES	17
COMBUSTOR PRESSURE POPPING	21
RESULTS AND CONCLUSIONS	28
REFERENCES	29
APPENDIX A	30

SUMMARY

An experimental study was conducted to study the spray formed by impinging streams of liquid hydrazine and nitrogen tetroxide. The experimental technique was based on photographic observation of the resulting liquid spray. Single exposure color photographs and high speed motion pictures with simultaneous chamber pressure traces recorded on the film were used.

Stream mixing and separation phenomena were determined based on the photographic observations. At low chamber pressures, the boiling of nitrogen tetroxide was found to play a significant role. With nitrogen tetroxide above the boiling point the resulting spray pattern showed that most of the liquid hydrazine was confined within the fuel side and thus resulted in very poor mixing. At high chamber pressure, separated flow was also observed. The resulting spray definitely showed a color variation with colorless hydrazine mainly on the fuel side of the spray and liquid nitrogen tetroxide on the oxide side. Good liquid spray mixing was observed at lower pressures. Propellant temperatures and jet diameter to velocity ratio appeared to be unimportant. Propellant additive also did not influence mixing at 15 Psia.

The occurrence of combustor pressure popping (sudden rise in chamber pressure which accompanied rapid burning of the liquid) was also found to depend on chamber pressures. Using .055" and .060" orifices, combustor pressure popping was very significant for chamber pressures below approximately 190 Psia and popping was rarely observed for chamber pressures above 190 Psia. Popping frequency and the average overpressure attained lower values at higher chamber pressures. Injector orifice played a significant role. Using .027" orifice, injector poppings were not observed and for .040" orifice, poppings were only observed infrequently under atmospheric pressures and were absent at high chamber pressures. To summarize, injector poppings occurred more frequently using larger orifice diameters at lower chamber pressures and less frequently using smaller orifice diameters at higher chamber pressures.

INTRODUCTION

Cold flow tests have been conducted to understand and to improve injector design technology. After very extensive studies of the resulting sprays formed by impinging chemically nonreactive streams, Rupe (Ref. 1) formulated an optimum mixing criteria. With impinging streams of real propellants, significantly different phenomena are observed, namely separation. As first reported by Elverum and Standhammer (Ref. 2) reactions of hypergolic propellants were rapid enough to prevent normal liquid phase mixing. These separation effects were particularly evident with hydrazine/nitrogen tetroxide systems. Continued experimental studies by Johnson (Ref. 3) and Evans, Stanford, and Riebling (Ref. 4) have shown reduced rocket engine performance with stream separation.

Photographic observations of stream separation phenomena were first conducted at NASA Lewis Research Center by Burrows (Ref. 5). Subsequent photographic studies of the resulting sprays were carried out at Dynamic Science (Refs. 6 and 7) to arrive at more quantitative data of the stream impingement phenomena. A slot injector was used with the resulting spray flowing over a lucite plate. Additional photographic observations have also been carried out at Rocketdyne (Ref. 8) and Aerojet (Ref. 9). An alternate method of using on-line mass spectrometer to study stream separation is being conducted by Houseman (Ref. 10).

Attempts to correlate and to predict stream separation phenomena have also been carried out. Separation criteria have been defined in terms of chemical reaction time and interface propellant residence time (Ref. 6). Kushida and Houseman (Ref. 11) proposed two complementary theoretical models; one based on the attainment of bubble point temperature, and a second model more applicable for higher pressures emphasized the gas phase reactions.

In addition to stream mixing and separation phenomena, violent explosions of liquid propellant sprays, commonly known as poppings, have also been observed. The objective of the present work was to determine the governing factors affecting stream mixing/separation phenomena and the occurrence of popping and to define engine operating regions where these different combustion processes are most likely to occur. These results will be most helpful for design engineers.

EXPERIMENTAL APPARATUS

Combustion Chamber

Impingement experiments were conducted using a single element, like on unlike, combustion chamber as shown in Figure 1. The injector consisted of a pair of stainless steel tubings press fitted into an aluminum injector plate, (Fig. 2). The tubings protruded 1/4 inch from the plate. Orifice alignments were properly refined under cold flow conditions by manually adjusting the protruding tubes. The impingement angle was fixed at 60°. The distance between the center of the two orifices were four orifice diameters apart. The ratio of the orifice length to that of orifice diameter (L/D) was equal to 100. Four different injector orifices, with orifice diameter respectively equal to .027", .040", .055", and .060" were used throughout the experiment.

The injector plate was fitted over a test chamber consisting of a rectangular aluminum block with a cylindrical hole 2" by 4 3/8" along the center of the block. Two viewing windows, with window openings equaled to 1.7" diameter were used for lighting and photographic purposes. Quartz windows were used because they were more compatible with the propellants as well as better light transmission in the ultra-violet range: Copper nozzles were attached to the bottom end of the chamber. Six different copper nozzles, with nozzle diameters equal to 1.5", .600", .400", .283", 179", and .128" were used to vary the chamber pressures.

Propellant Feed System

A schematic of the nitrogen tetroxide/hydrazine flow system is shown in Figure 3. The flow systems were fabricated with 304 stainless steel lines. The propellant tanks were designed for a working pressure of 1000 Psia. The tank capacities were approximately 1/3 gallon. Pressurization of the tank was controlled by a regulator and a release valve which was set at 1000 Psia. Two solenoid valves were used to vary the dome pressure of the regulator. Propellant flow rates were controlled by the propellant tank pressure and also by variable area cavitating venturi valves. The flow controllers were micrometer head type. This device provided easy and precise control of the propellant flows and allowed for more efficient testing with the ability to match desired stream momentum ratios. Heat exchangers were provided for each of the propellant tanks, and coaxial lines were used for the entire propellant supply system. Propellant temperature was controlled by flowing water at elevated temperatures or ethylene glycol-water mixtures at low temperatures through the heat exchangers and the propellant coaxial feedlines. Two 500 watt heaters were used to raise the water temperatures. A refrigerated coil bath conditioner, with a refrigeration compressor unit was used to condition the ethylene glycol-water mixture temperatures. Propellant temperature variations between 40° F and 140° F could be easily attained using this system. Prior to each test, the propellants were first led into a by-pass tank until the desired propellant flow rate and temperature were achieved before being introduced into the combustion chamber.

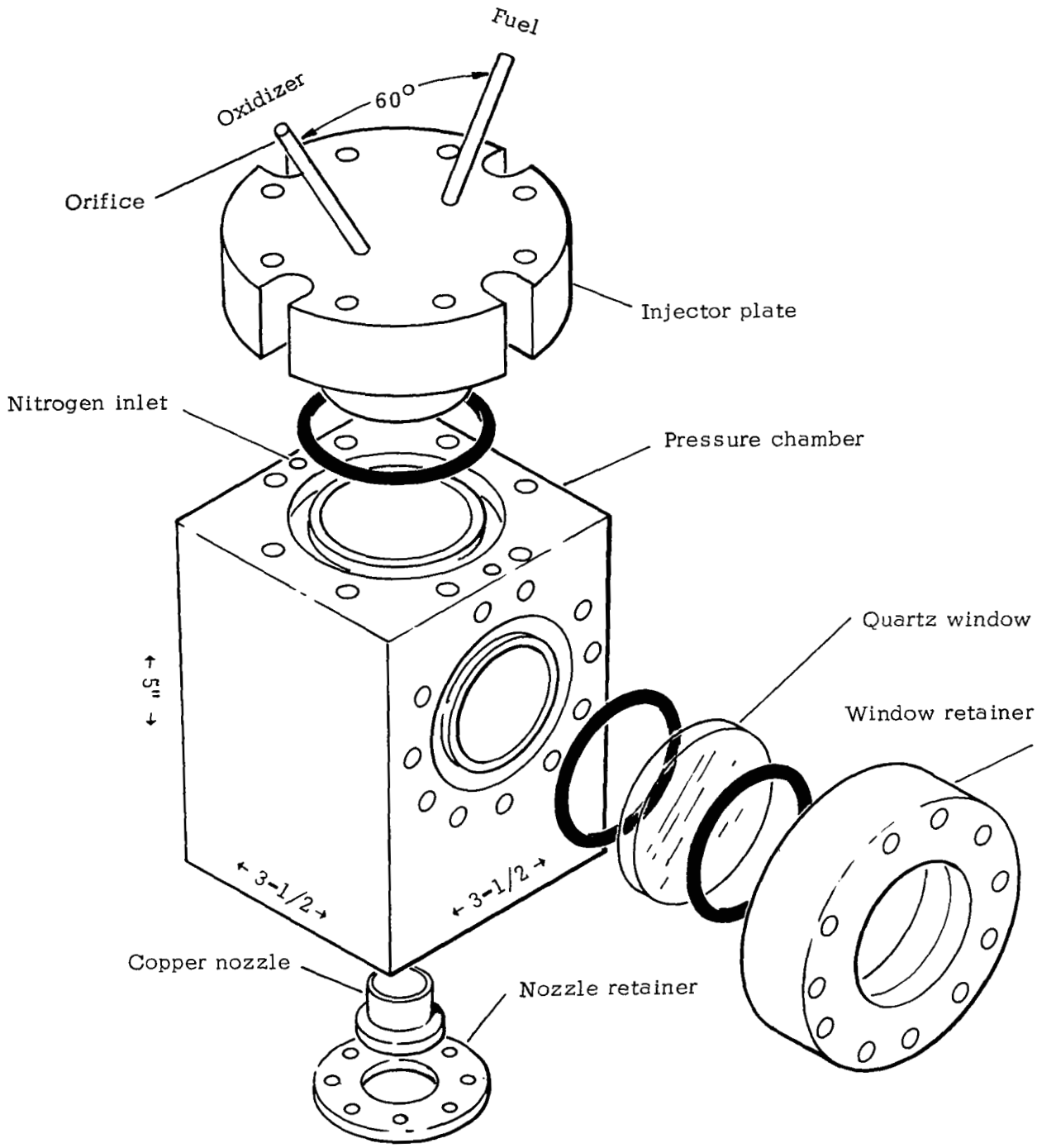

Figure 1. High Pressure Impingement Test Chamber.

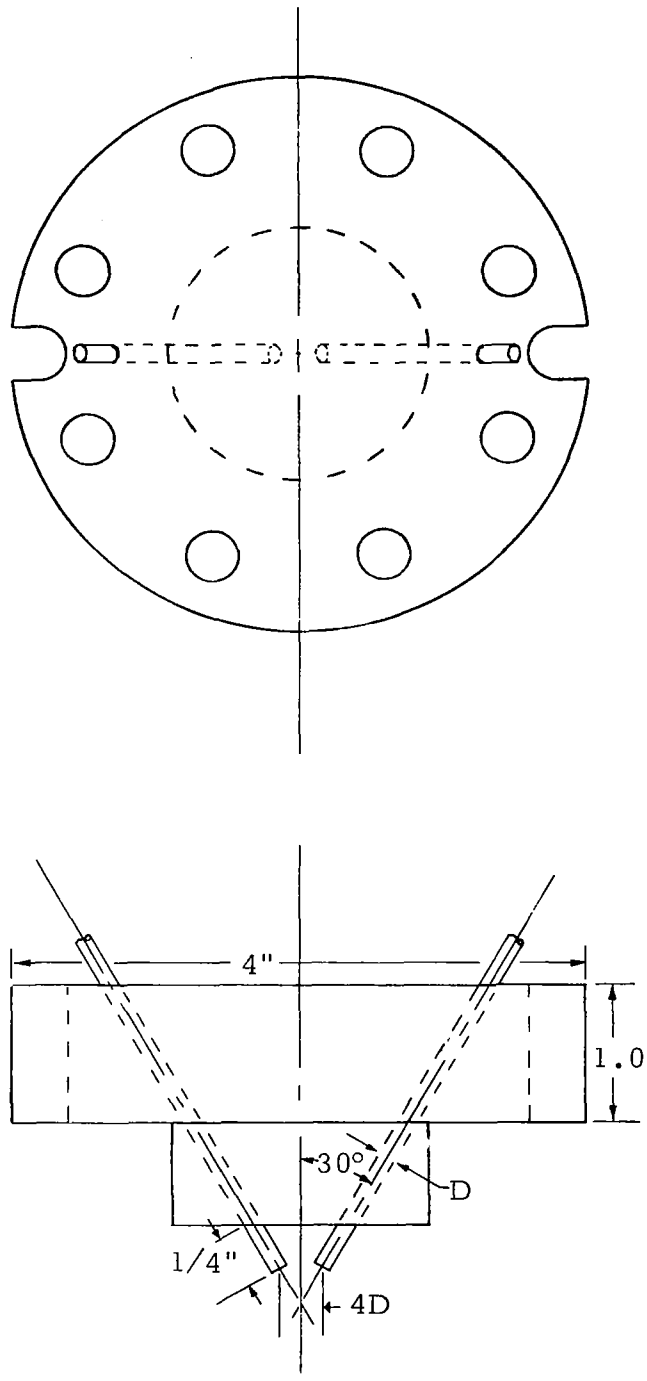

Figure 2. Injector Plate for Impingement Studies.

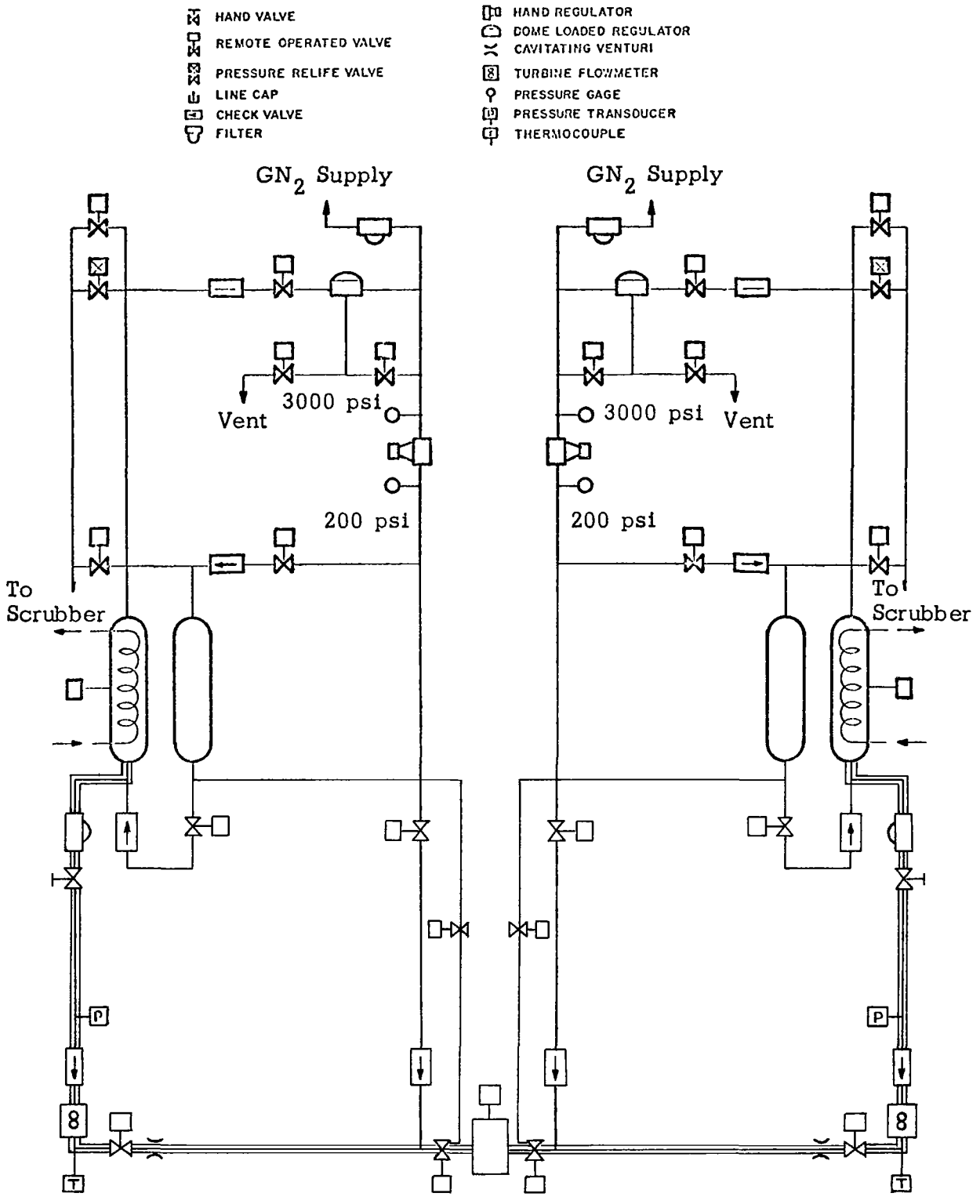

Figure 3. N_2O_4/N_2H_4 Flow System.

Recording Instrumentation

Hydrazine and nitrogen tetroxide flow rates were measured with turbine type flow meters. I/C thermocouples were used to record the propellant temperatures in the tanks; immediately downstream of the flow meters, and at the injectors. Propellant tank pressures were monitored by strain gauge transducers. Chamber pressures were measured with a quartz pressure transducer and a strain gauge transducer.

The test control console housed the propellant control console, a test sequence unit, amplifiers and various recording instrumentation and related components. The signals of the flow meters, thermocouples at the injectors, and pressure transducers of the combustion chamber were fed into amplifiers to a recording oscillograph. The flow rates were determined from the meter frequencies output and the propellant densities. An oscilloscope was also used in certain tests to record the pressure signal of the quartz transducer. Propellant tank pressures were recorded on a two channel strip recorder. Propellant temperatures in the tank and at the flow meters were recorded on a multipoint recorder. The entire experiment was operated remotely through the test control console.

Photography

The experimental technique was based on photographic observeration of the impingement region. Both single exposure photograph and high speed motion pictures were used. A microflash system was used to provide the proper lighting for single exposure photography. Flash duration was approximately 1.0 microsecond with peak light intensity of thirty million beam candlepower. This high intensity completely masked out the flame light, and the microsecond flash duration stopped the stream and droplets motion, thus allowing clear observation of liquid hydrazine and liquid nitrogen tetroxide. All of the single exposure photographs were recorded on color films.

The impingement phenomena were also recorded on high speed motion pictures. A rotating prism camera, with framing speed set at 3000, 4000, and mostly at 5000 frames per second was used. In addition, a shutter with an exposure ratio of 1/100 was also employed so that a two microsecond exposure time was obtained with a framing speed of 5000 per second. To observe injector poppings, it was most desirable to correlate the chamber pressures with that of the explosion phenomena. To best achieve this correlation, the output of the quartz transducer was fed into an oscilloscope and the film was back-exposed with the oscilloscope trace. Thus the high speed motion pictures simultaneously recorded the injector poppings and the corresponding pressure spikes. Figure 4 shows the experimental setup where a second lens was attached to the backside of the movie camera and was used to focus the chamber pressure traces on the oscilloscope.

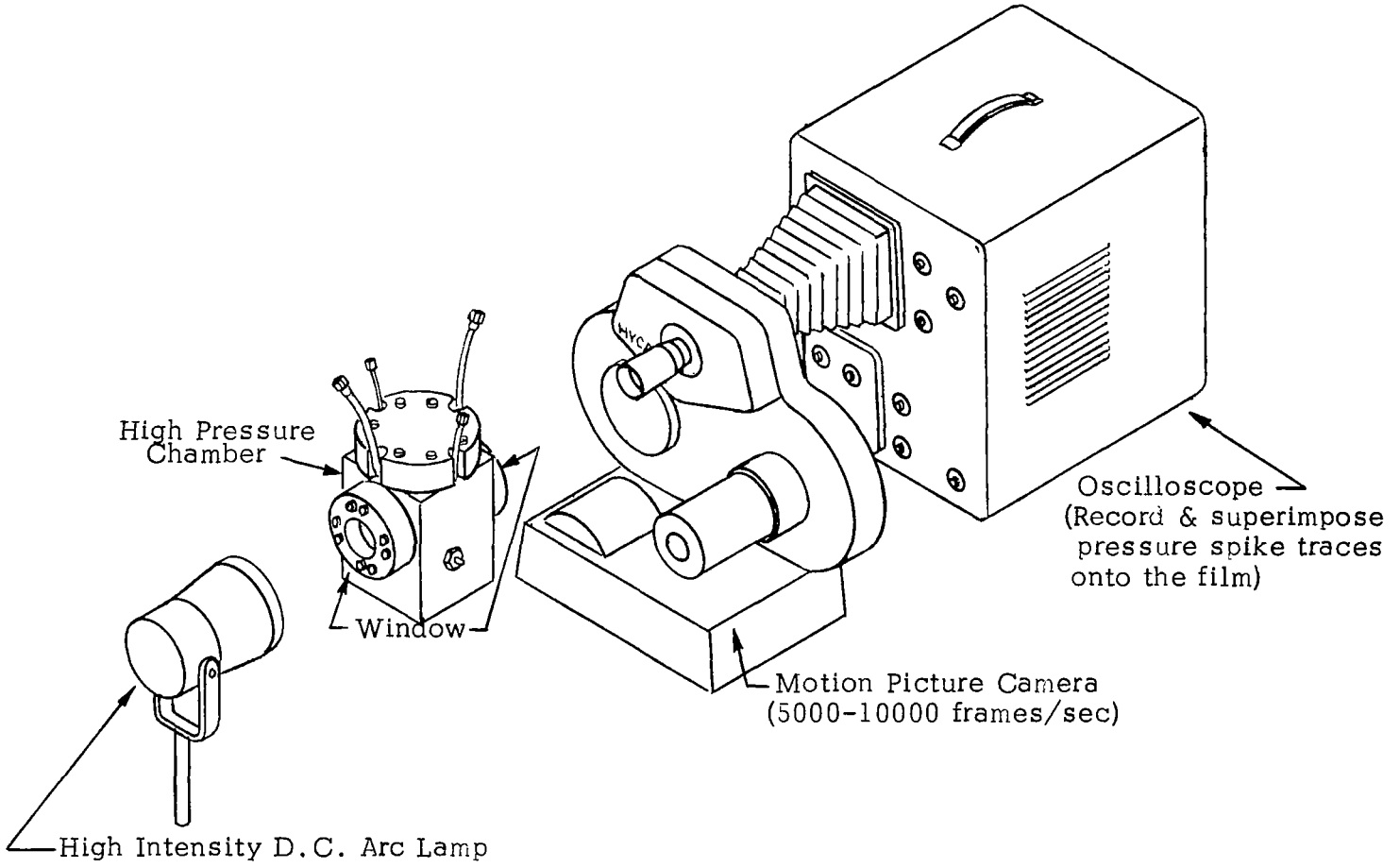

Figure 4. Experimental Setup for Studying Injection Mixing Explosions.

IMPINGEMENT EXPERIMENTS UNDER ATMOSPHERIC PRESSURE

Tests were conducted by impinging liquid streams of hydrazine and nitrogen tetroxide either in the open atmosphere or within the combustion chamber using a 1 1/2 inch diameter nozzle. The latter technique was desirable to protect the photographic instrumentation when closer observations were required. Only single exposure photography was employed during this phase of study. Results were analyzed based on the photographic observations of the spray by impinging streams of hydrazine and nitrogen tetroxide. The test parameters for this phase of study were as follows:

Chamber Pressure	:	one atmosphere
Propellant Temperature		
Hydrazine	:	45°F - 105°F
Nitrogen Tetroxide	:	42°F - 80°F
Propellant Velocity		
Hydrazine	:	18 ft/sec - 94 ft/sec
Nitrogen Tetroxide	:	16 ft/sec - 72 ft/sec
Orifice Diameters (inch)	:	.027, .040, .055, .060.

Two distinctly different impingement phenomena were observed under atmospheric pressure tests. For nitrogen tetroxide temperature above the boiling point ($\approx 70°F$), vaporization of the oxidizer was significant, resulting more closely to a gas/liquid impingement. For nitrogen tetroxide temperature below the boiling point, liquid/liquid impingement was observed. Figure 5* shows a photograph of a gas/liquid impingement. The flash light intensity (30 million beam candles) completely masked out the flame. The short flash duration (1.0 μ second) stopped the motion of propellant droplets and ligaments. The presence of the oxidizer vapor was evidenced by the slight spreading of the jet, with the flow velocity mainly along the injector axis. The nitrogen tetroxide vapor attained a much higher velocity as compared with that of liquid hydrazine. The resulting vapor stream carried the hydrazine droplets along with it, confining the hydrazine droplets mainly on the fuel side. This corresponded to a "separated" flow. Figure 6 is the photograph of the identical flow situation. The photograph was taken with 0.5 second exposure time without the flash and thus showed the combustion flames of the impingement region. The flame light indicated that the combustion occurred mainly on the hydrazine side, similarly indicating a "separated" flow.

*Color photographs are presented in film supplement C-273 to this report, which is available on load; a request card and a description of the film are included at the back of the report.

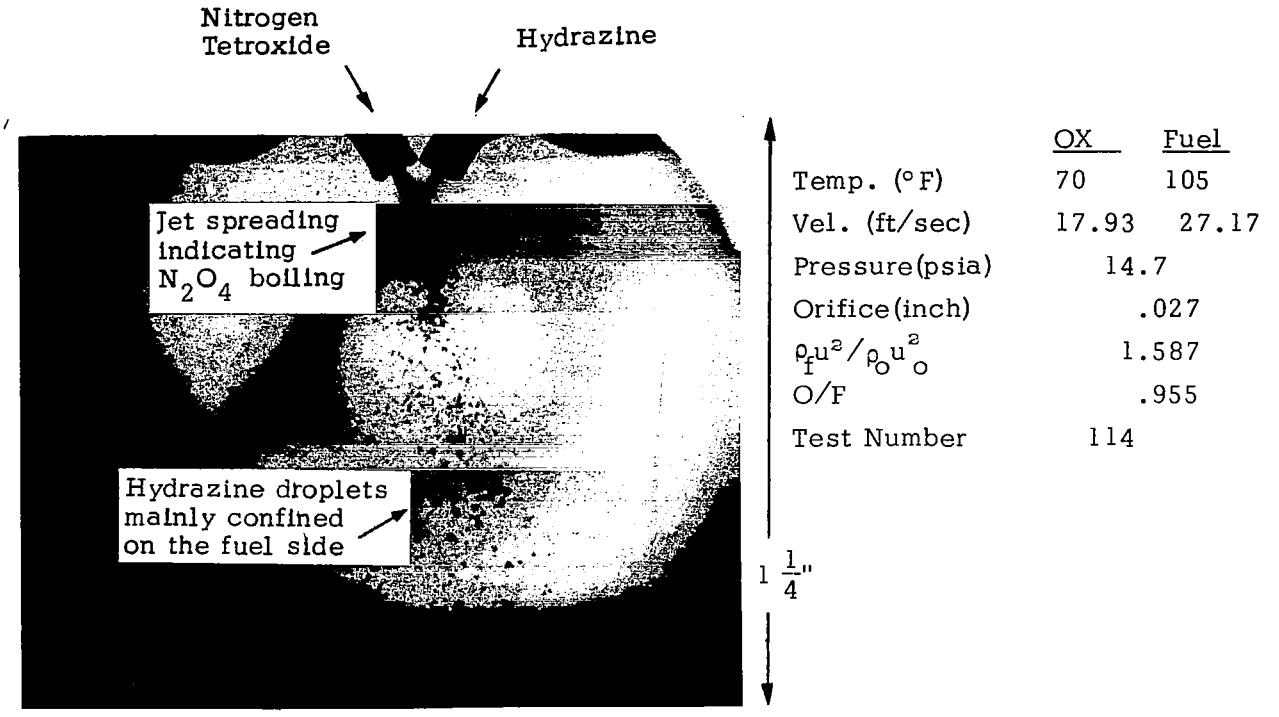

Figure 5. Stream Separation With Two Phase N_2O_4 Stream.

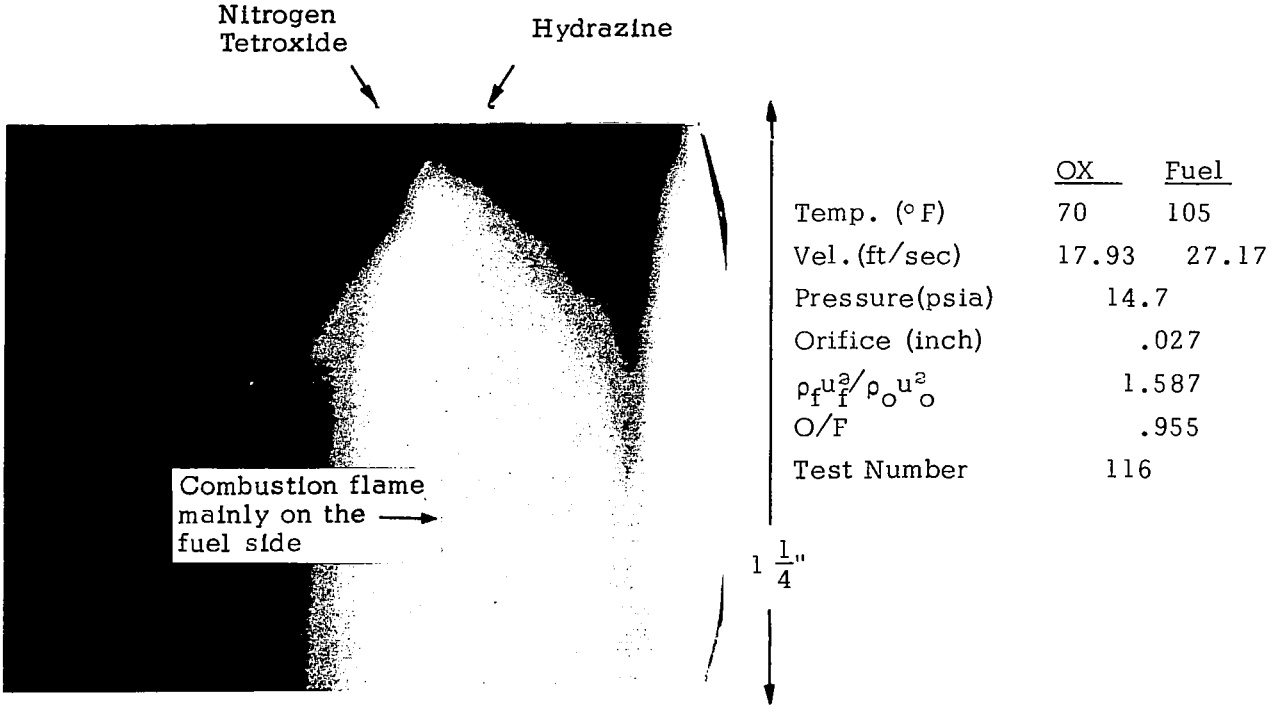

Figure 6. Time Exposure Photograph of Stream Separation with Two Phase N_2O_4 Stream.

For nitrogen tetroxide temperature below 70°F, liquid/liquid stream impingement was observed. The color of the resulting spray was very uniform showing that droplets and ligaments of liquid fuel and liquid oxidizer were intermixed. Figure 7 is an illustration of the stream mixing case.

Figure 8 shows the result of the impingement study under atmospheric pressure conditions. The data are presented in terms of D/V (the ratio of orifice diameter to average propellant velocity) and the temperature of nitrogen tetroxide at the injectors. The data indicated that for nitrogen tetroxide temperature above approximately 70°F, very poor liquid mixing occurred due to the vaporization of nitrogen tetroxide stream as discussed previously. For nitrogen tetroxide temperature below approximately 70°F, the resulting spray showed good mixing of the liquid propellants. Injector popping was also observed within these temperature ranges. The simultaneous occurrence of both popping and stream mixing will be discussed in more detail in the injector popping section of this report.

Effect of unequal propellant temperatures on stream mix/separation phenomena was also studied under atmospheric pressure conditions. The result presented in Figure 9 indicated that hydrazine temperature played no significant role. Influence of unequal propellant velocities was also found to be insignificant when approximately equal temperature streams of hydrazine and nitrogen tetroxide impinged at atmospheric pressures. Effects of additives were also evaluated and found to be unimportant. 1% and 5% of unsymmetric dimethylhydrazine, monomethylhydrazine and ammonium nitrate were respectively added to liquid hydrazine and no significant influence on stream mixing and separation was observed.

In conclusion, under atmospheric pressures, the temperature of nitrogen tetroxide streams played the dominant role with respect to stream mixing and separating phenomena. Stream separation was never observed when nitrogen tetroxide was below its boiling point. For nitrogen tetroxide above the boiling point, stream separation occurred due to vapor/liquid impingement. Effects of unequal stream velocities, unequal propellant temperatures, and various additives in hydrazine were found to be insignificant.

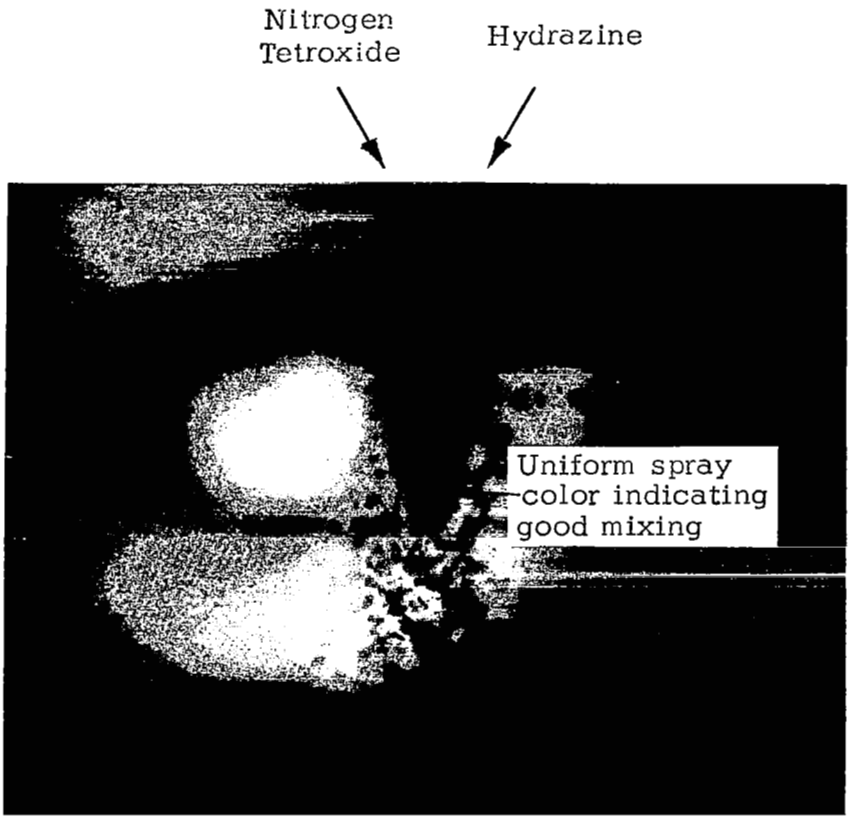

	OX	Fuel
Temperature (^{O}F)	54	54
Velocity (ft/sec)	11.85	14.49
Pressure (Psia)	14.7	
$\rho_f u^2_f / \rho_o u^2_o$	1.17	
Orifice (inch)	.060	
Run No.	136	

Figure 7. Example of Stream Mixing with Liquid/Liquid Impingement.

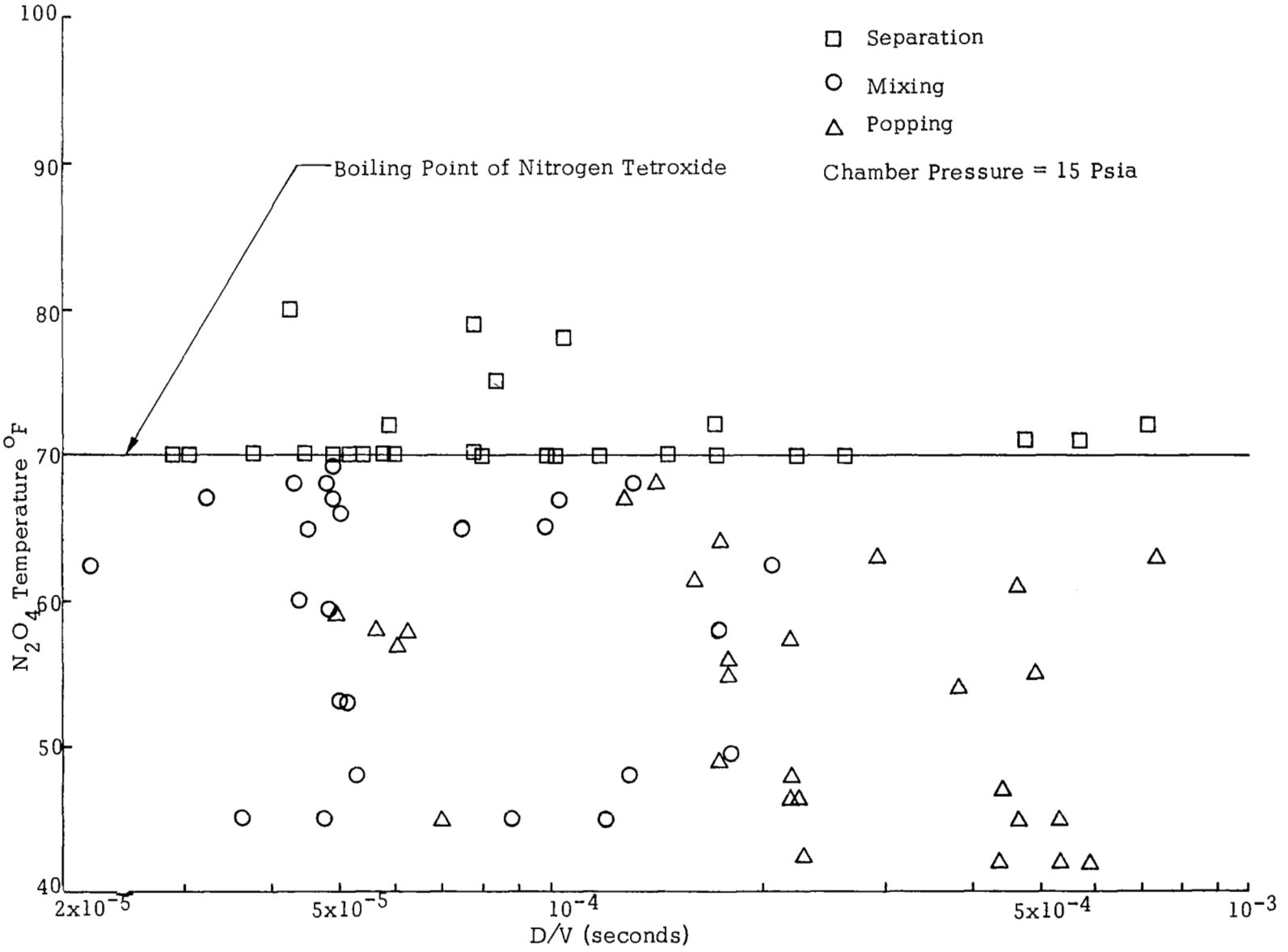

Figure 8. Nitrogen Tetroxide-Hydrazine Stream Impingement Data.

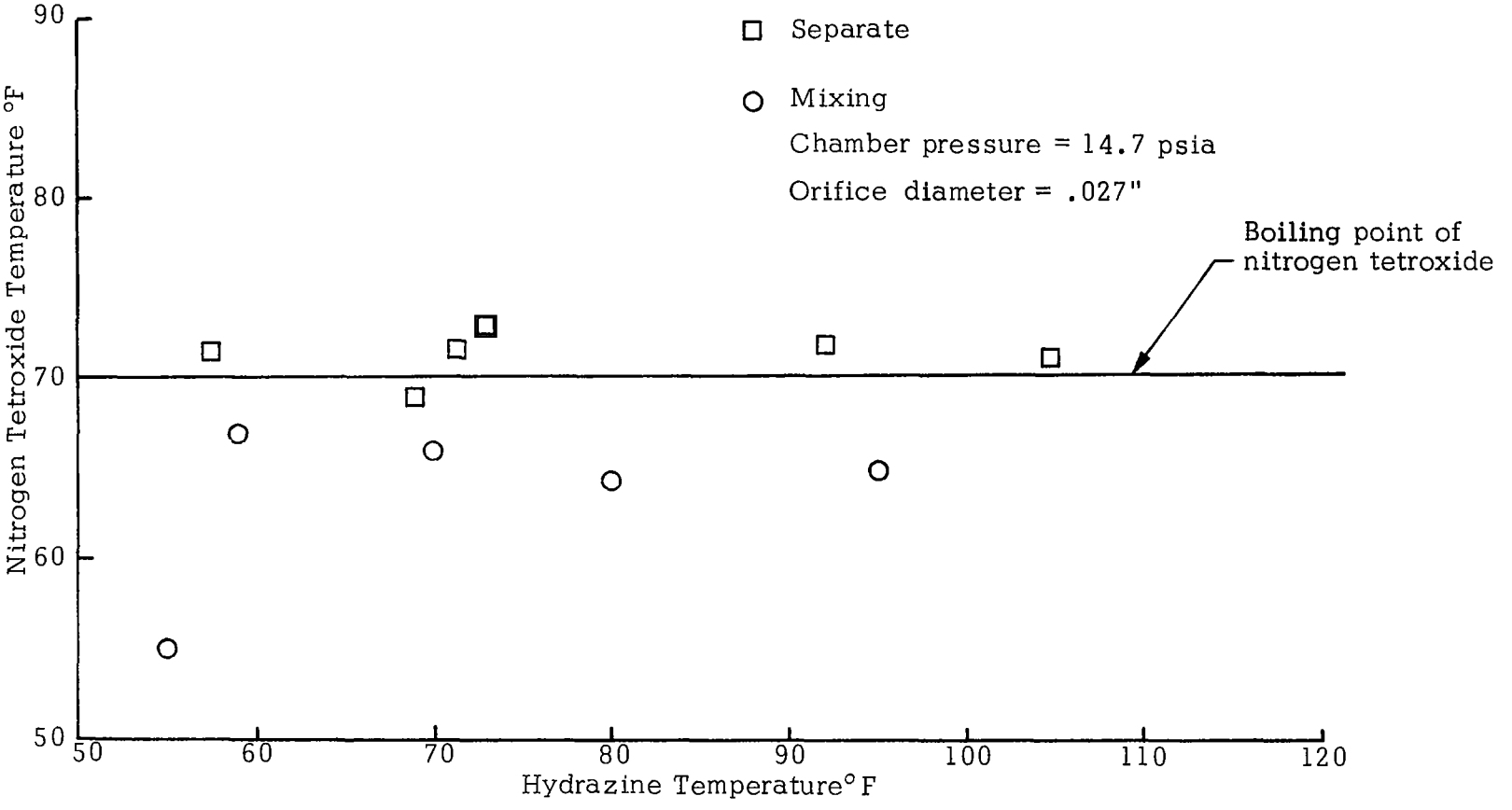

Figure 9. Effect of Propellant Temperature Difference on Stream Mixing and Separation. $(.95 < \frac{\rho_f u_f^2}{\rho_o u_o^2} < 1.05)$

Comparison With Previous Experimental Studies

Impingement experiments have been previously conducted (Ref. 6) using a different injector system. It consisted of an aluminum block with orifice slots on which a lucite observation window was bolted with a heavy retaining plate. The block was cut away at the impingement point to allow fan formation away from the lucite window. This injector design was different from the existing setup in two ways. First, the propellants were led to flow over the lucite plate so that the lucite burning could affect the photographic observations especially when photographs were obtained from the lucite view of the injector. Second, the impingement occurred at the immediate exit of the orifice, with no provision for jet free travel. The photographic observations of the impingement region used a 10μ second duration strobe back-lighting. Photographs of the combustion flames with 0.5 second exposure time without flash backlighting were also carried out.

The experimental data previously obtained (Fig. 10) in general, agreed very well with that shown in Figure 8. The limiting boundary line (Fig. 10) separating regions of separation with that of mixing and popping was indeed close to the boiling point of nitrogen tetroxide. Based on the mixing and separation criterion previously defined (Ref. 6), stream separation was attributed to tremendous gas release associated with chemical reactions. The present study suggested that stream separation was mainly due to the boiling of the nitrogen tetroxide stream. To resolve this disagreement, experiments were performed using the slot injector with the lucite plate. High speed motion pictures, with a 2.0μ second exposure time per frame were used to observe the impingement region. A significant amount of oxidizer gas was observed under previously separated conditions, indicating that the separation phenomena could be caused by the boiling of nitrogen tetroxide rather than due to reactions at the interface between propellants.

In summary, the previously proposed mixing/separation criteria of Reference 6 in the temperature ranges where propellant boiling was significant, has to be modified. Furthermore, under the temperature and pressure conditions where separation was observed, further experimental work indicated that separation was attributed to the boiling of nitrogen tetroxide resulting in gas/liquid impingement and thus produced very poor propellant mixing.

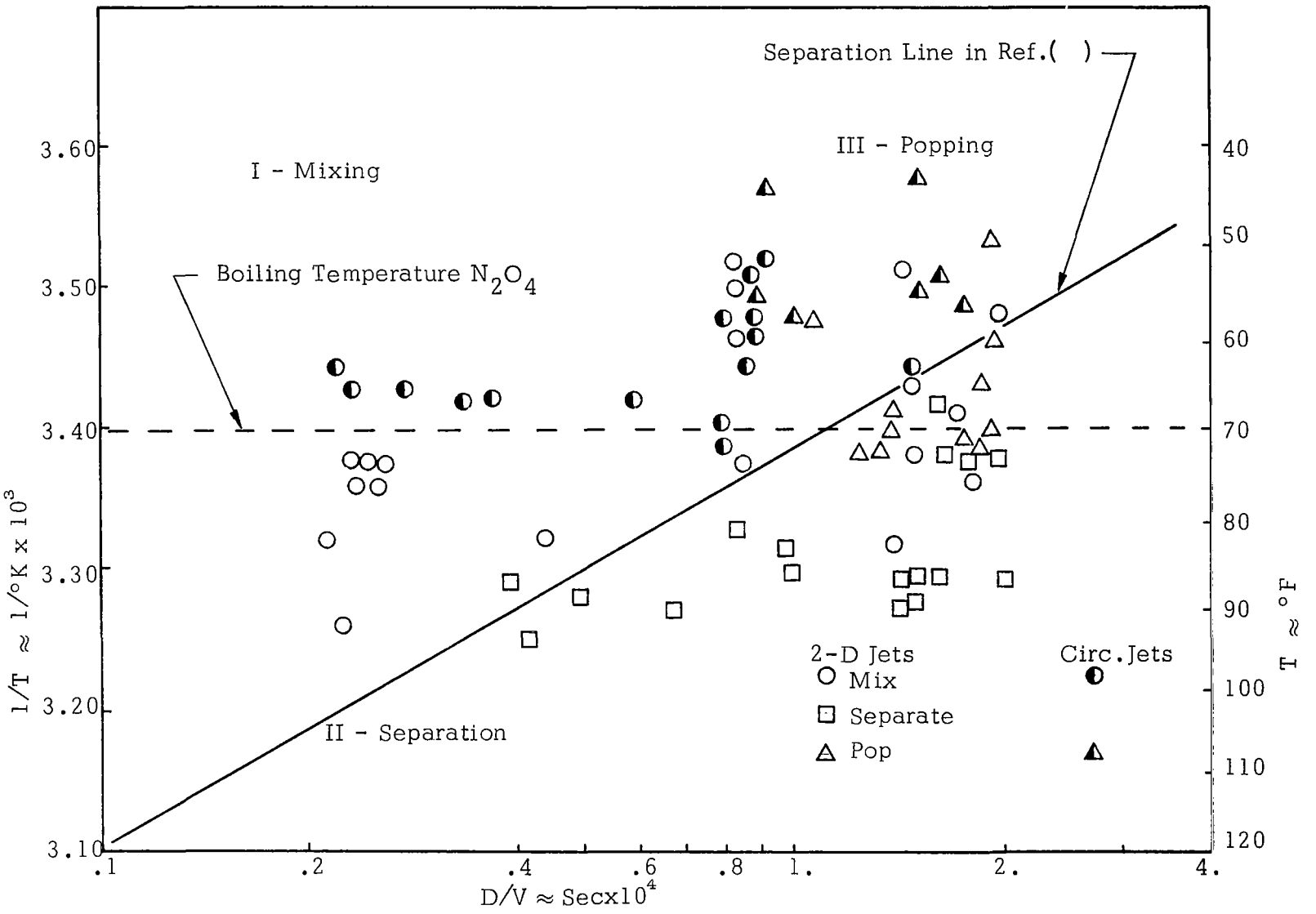

Figure 10. Impinging Jet Separation Data for N_2O_4/N_2H_4 Streams, From Ref. (6).

STREAM MIXING/SEPARATION RESULTS AT ELEVATED CHAMBER PRESSURES

Stream mixing and separation phenomena at elevated pressures were studied by impinging liquid hydrazine and nitrogen tetroxide within a pressure test chamber (Figure 1). The experimental conditions were as follows:

Chamber pressure	:	15 Psia - 500 Psia
Propellant Temperature		
Hydrazine	:	$40^{o}F$ - $140^{o}F$
Nitrogen Tetroxide	:	$40^{o}F$ - $140^{o}F$
Propellant Velocity		
Hydrazine	:	15 ft/sec - 90 ft/sec
Nitrogen Tetroxide	:	15 ft/sec - 80 ft/sec
Orifice Diameters	:	.040" - .055"
Nozzle Diameters	:	1.5", .600", .400", .283", 179", and .128".

Single exposure color photography and high speed color motion pictures were employed during this phase of study. For single exposure photography a high intensity, microsecond duration flash was used. A high intensity tungston lamp was used to provide proper lighting for high speed motion picture observations. With a 1/100 exposure ratio shutter, a two microsecond exposure time was obtained with a framing speed of 5000 per second. The high intensity lighting technique completely masked out the flame light, and the microsecond exposure time, (1.0μ second for single exposure and 2.0μ second for high speed motion pictures) stopped the liquid stream and droplet motion, thus allowing clear observation of liquid hydrazine and liquid nitrogen tetroxide. The colors of the two impinging streams were distinguishable; hydrazine being colorless and nitrogen tetroxide being darkish brown. Mixing and separation phenomena were determined based on the color distinction of the two liquid propellants within the spray. For sprays with uniform brownish color, the impingement phenomenon was defined as mixed. Whenever color variations within the sprays were observed, with colorless liquid hydrazine along the fuel side of the spray, the impingement phenomenon was defined as "separated."

Figure 11 is a photograph of a mixed spray resulting from impinging liquid hydrazine stream with that of nitrogen tetroxide. The color of the spray was very uniform, indicating good intermixing of droplets and ligaments of two liquid propellants. Figure 12 is an illustration of poor propellant mixing. The color variation within the spray indicated that most of the colorless liquid hydrazine remained on the fuel side while brownish liquid nitrogen tetroxide mainly remained on the oxide side.

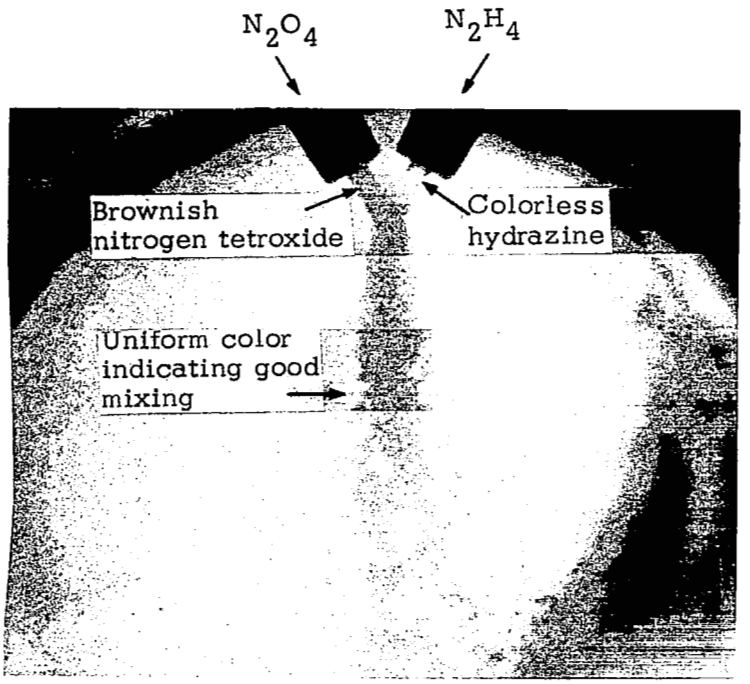

	OX	Fuel
Temp (°F)	100	71
Velocity (ft/sec)	54.8	46.2
Pressure (Psia)	162	
$\rho_f u_f^2 / \rho_o u_o^2$	.98	
O/F	1.24	
Orifice	.040"	
Nozzle	.283"	
Test Number	242	

Figure 11. Typical Spray Photograph for Stream Mixing at High Pressure.

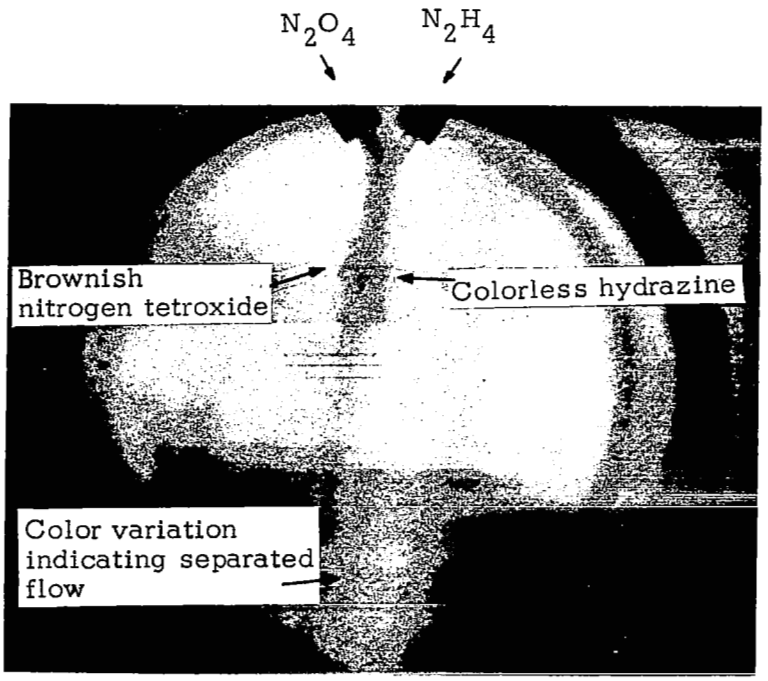

	OX	Fuel
Temp (°F)	93	104
Velocity (ft/sec)	31.66	36.76
Pressure (Psia)	422.7	
$\rho_f u_f^2 / \rho_o u_o^2$	.95	
O/F	1.22	
Orifice	.040"	
Nozzle	.128"	
Test Number	259	

Figure 12. Typical Spray Photograph for Stream Separation at High Pressures.

This is an example of poor intermixing of droplets and ligaments of two liquid propellants and is defined as "separated" flow. High speed motion pictures of the sprays with very similar flow conditions as those shown by Figure 11 and Figure 12 were also recorded. It was difficult to distinguish the propellant colors since a high intensity tungston filament lamp was used to provide the backlighting. The motion pictures did show one distinct feature. Brownish oxidizer vapor was found on both sides of the resulting spray in the stream mixed case while oxidizer vapor was found to be more noticeable on the nitrogen tetroxide side of the spray in the stream separated case.

At low chamber pressures (under 60 Psia) vaporization of nitrogen tetroxide was again found to play a significant role. Separated flows due to gas/liquid impingement were observed. As evidenced by Figure 5 and Figure 12, the sprays of the two "separated" flows were significantly different.

Stream mixing/separation results at elevated chamber pressures are shown in Figure 13. Test data presented were only those with chamber pressure fluctuations less than 5%. In terms of average initial propellant temperatures and chamber pressures, two different separated flow regions were defined (shaded regions in Fig. 13). Separated flows were observed for chamber pressures above approximately 230 Psia. The color photographs of these sprays definitely showed a color variation with liquid hydrazine appearing on the fuel side of the spray. The effects of initial propellant temperature and injection velocities were found to be not significant, (similar to Fig. 12). At lower chamber pressure (less than $\approx$ 230 Psia) and for nitrogen tetroxide below its boiling point, sprays with very uniform brownish color were observed. These were the mixed flows. At chamber pressures below 60 Psia and for initial nitrogen tetroxide temperature above the boiling point, separated flows as a result of gas/liquid impingement, were observed. The data agreed very well with the nitrogen tetroxide vapor pressure curves. For chamber pressure at 55 Psia, gas/liquid impingement was observed for nitrogen tetroxide temperature above 133°F, resulting in a spray pattern similar to that shown in Figure 5. The effect of different propellant velocities was found to be not significant.

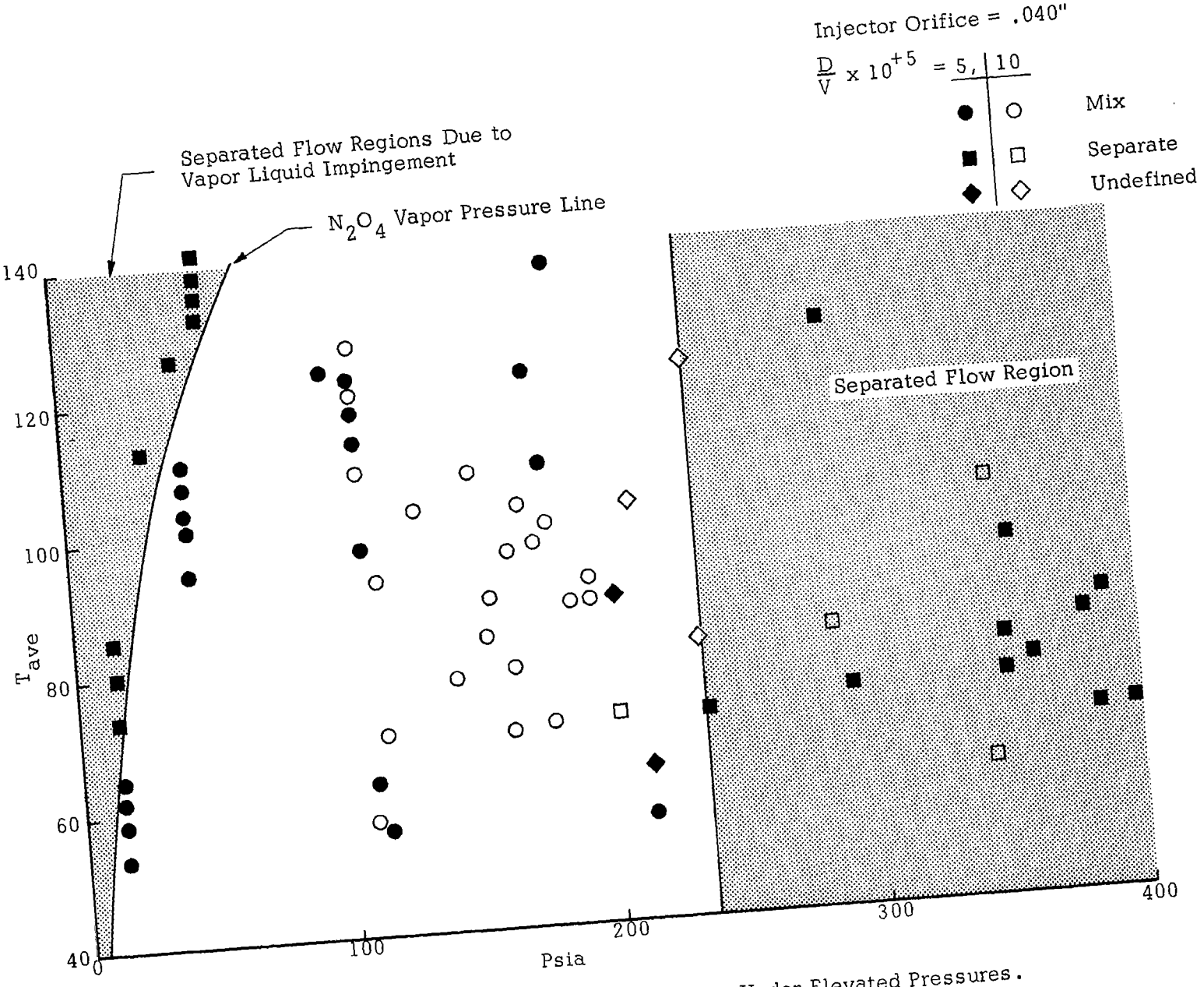

Figure 13. Region of Stream Mixing and Stream Separation Under Elevated Pressures.

COMBUSTOR PRESSURE POPPING

Transient high amplitude pressure disturbances, commonly referred to as "pops" have been observed during steady state rocket engine operation. The term "pop" has also been used to describe altitude ignition spikes and shutdown spikes. In the present discussion, the term popping will be used to describe high pressure disturbances associated with a single doublet injector element during steady state engine operation conditions.

Popping was studied under atmospheric and elevated pressures with impinging liquid streams of hydrazine and nitrogen tetroxide. The occurrence of popping was particularly easy to distinguish when impingement experiments were conducted in the open atmosphere. This was evidenced by the loud noise associated with these explosions. The noise of these explosions was recorded on the oscillograph via a microphone. Popping studies under elevated pressures were investigated by impinging propellant streams within the combustion chamber as shown in Figure 1. High speed motion picture technique was used to observe the popping. Chamber pressures were simultaneously recorded on the oscillograph and on the movie film via an oscilloscope. The occurrence of popping was determined based on motion picture observations and the related pressure spikes.

Experimental results showed that the two dominant parameters governing the occurrence of popping are the orifice injector diameter and the chamber pressure. Under atmospheric pressure with nitrogen tetroxide temperature below its boiling point, test results showed that popping was never observed when .027" diameter injector was used. Popping was observed infrequently when .040" diameter was used. Popping was always observed when .055" and .060" diameter orifices were used.

A typical occurrence of popping is illustrated in Figure 14. The photographs were reproduced from motion picture recordings. The film speed was 5280 frames per second. With the addition of a 1/100 exposure ratio shutter, the exposure time was approximately 2.0μ seconds. The experimental conditions were:

Chamber Pressure	:	100 Psia
Propellant Temperature		
Hydrazine	:	71.5^{o}F
Nitrogen Tetroxide	:	68.0^{o}F
Propellant Velocity		
Hydrazine	:	52.8 ft/sec
Nitrogen Tetroxide	:	46.5 ft/sec
Orifice Diameter	:	.060"

t = 0.0 sec., P_c = 100 psia

t = 1326μ sec., P_c = 190 psia

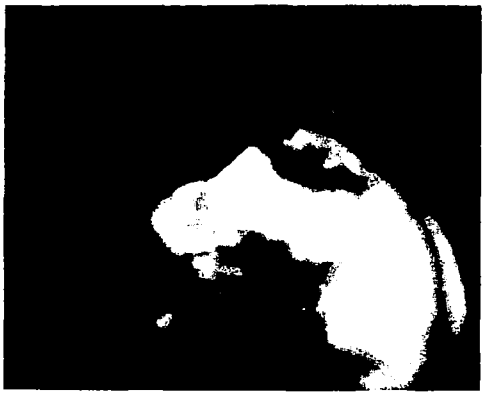

t = 189μ sec., P_c > 475 psia

t = 1894μ sec., P_c = 175 psia

t = 757μ sec., P_c > 475 psia

t = 3409μ sec., P_c = 100 psia

Figure 14. Hydrazine/Nitrogen Tetroxide Injector Popping Sequence. Test Number 479. Steady State Chamber Pressure = 100 psia.

The pressure spike associated with the popping at a time of 189μ seconds in Figure 14, was in excess of 475 Psia. The entire popping sequence took approximately 3000μ seconds.

By increasing the chamber pressure to approximately 195 Psia (by replacing the chamber nozzle from .600" to .400") high pressure spikes were no longer recorded on the oscillograph results. The corresponding high speed motion picture recordings also did not show the violent explosion disturbance of popping. Only intermittant stream blow aparts were observed. These blow aparts did not produce any appreciable pressure spikes, but did produce chamber pressure fluctuations of approximately 10%. Figure 15 is a typical sequence of this blow apart phenomenon. The experimental conditions were:

Chamber Pressure	:	195 Psia
Propellant Temperature		
Hydrazine	:	70^{o}F
Nitrogen Tetroxide:		68^{o}F
Propellant Velocity		
Hydrazine	:	51.0 ft/sec
Nitrogen Tetroxide	:	46.5 ft/sec
Orifice Diameter	:	.060"

These tests showed that poppings which were observed with chamber pressure at 100 Psia were no longer observed with chamber pressure at 195 Psia. Color movies of popping (Fig. 14) and absence of popping (Fig. 15) are shown in the film supplement to this report.

The effect of chamber pressure can be briefly summarized as follows: at higher chamber pressures (Pc > 40 Psia) popping was not observed for both .027" and .040" diameter orifices. For .055" and .060" diameter orifices, popping was rarely observed when chamber pressures were above 185 Psia. The effect of chamber pressure and orifice diameter on the occurrence of popping is shown in Figure 16. It has been observed that popping was more likely to occur for large orifice diameter at lower chamber pressures and less likely to occur for smaller orifices and at higher chamber pressures. Both propellant temperature and velocity were found to be not important.

Popping frequency and average pressure spikes were obtained from the oscillograph data. These results are shown in Figure 17 and 18. Although the data were not reproducible, it did show the effect of pressure. Both the popping frequency and the magnitude of the pressure spikes are higher at lower chamber pressures.

t = 0.0 second

t = 600 microsecond

t = 200 microsecond

t = 800 microsecond

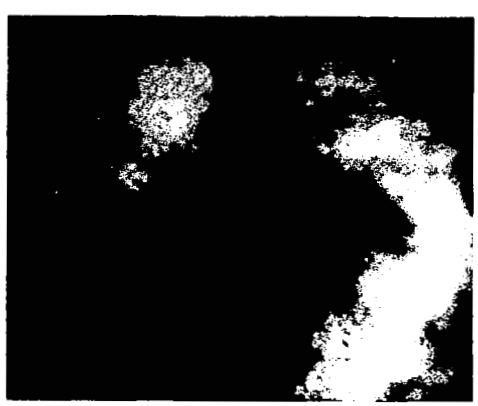

t - 400 microsecond

t - 1000 microsecond

Figure 15. Hydrazine/Nitrogen Tetroxide Blow Apart Phenomena. (Test number 386, Steady State Chamber Pressure = 195 psia).

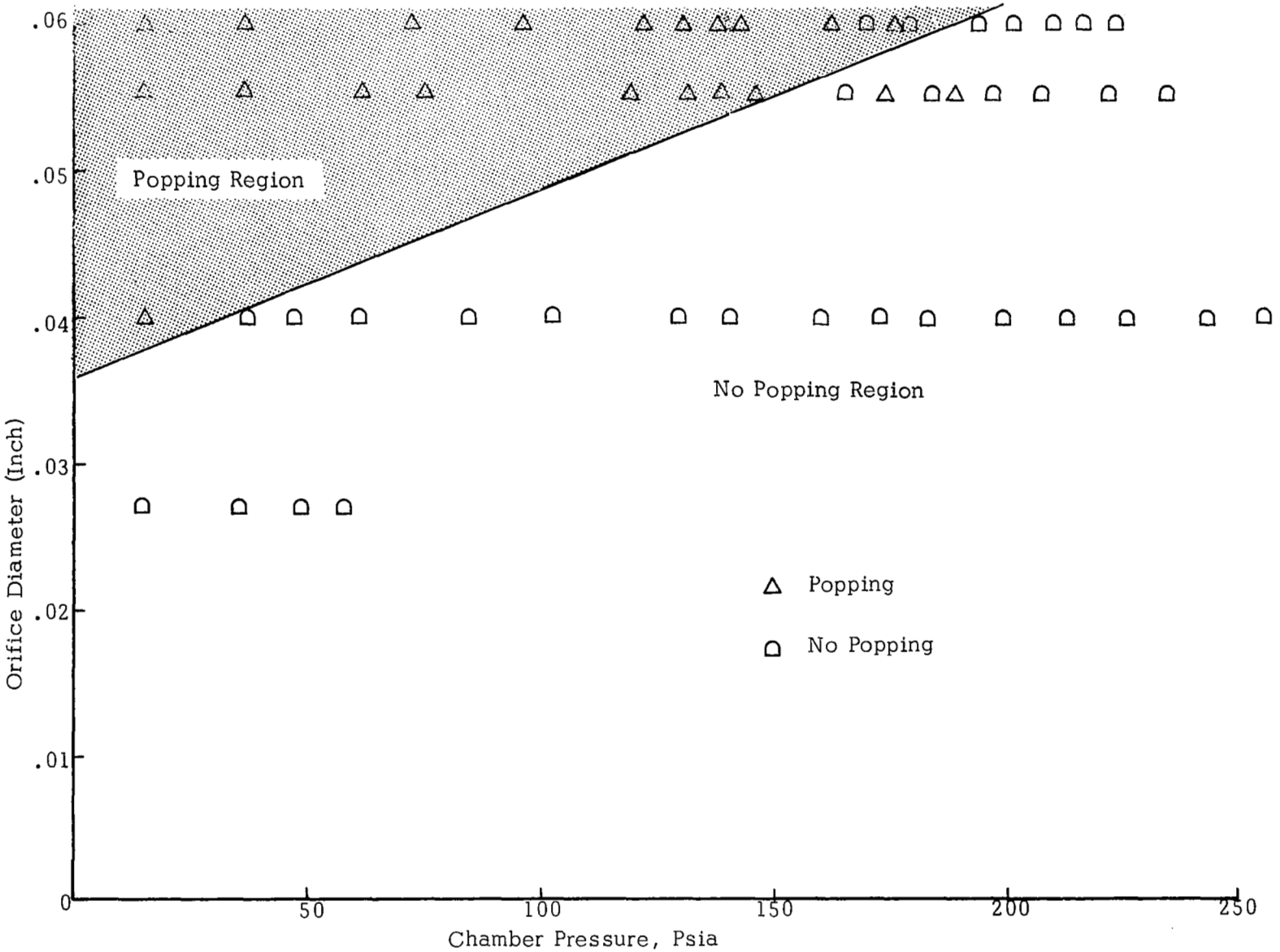

Figure 16. Hydrazine/Nitrogen Tetroxide Popping Regions.

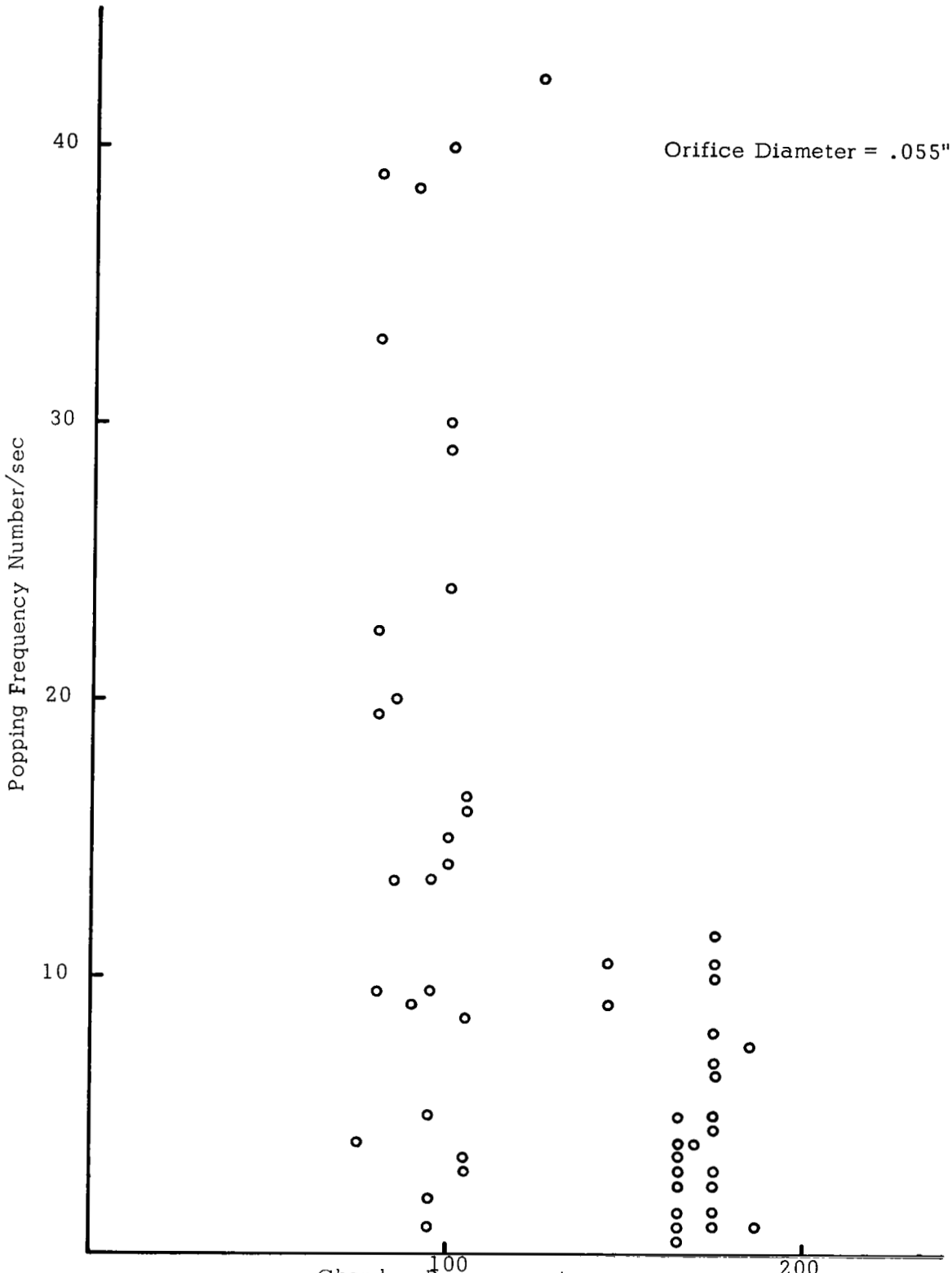

Figure 17. Variation of Popping Frequency for Different Chamber Pressures.

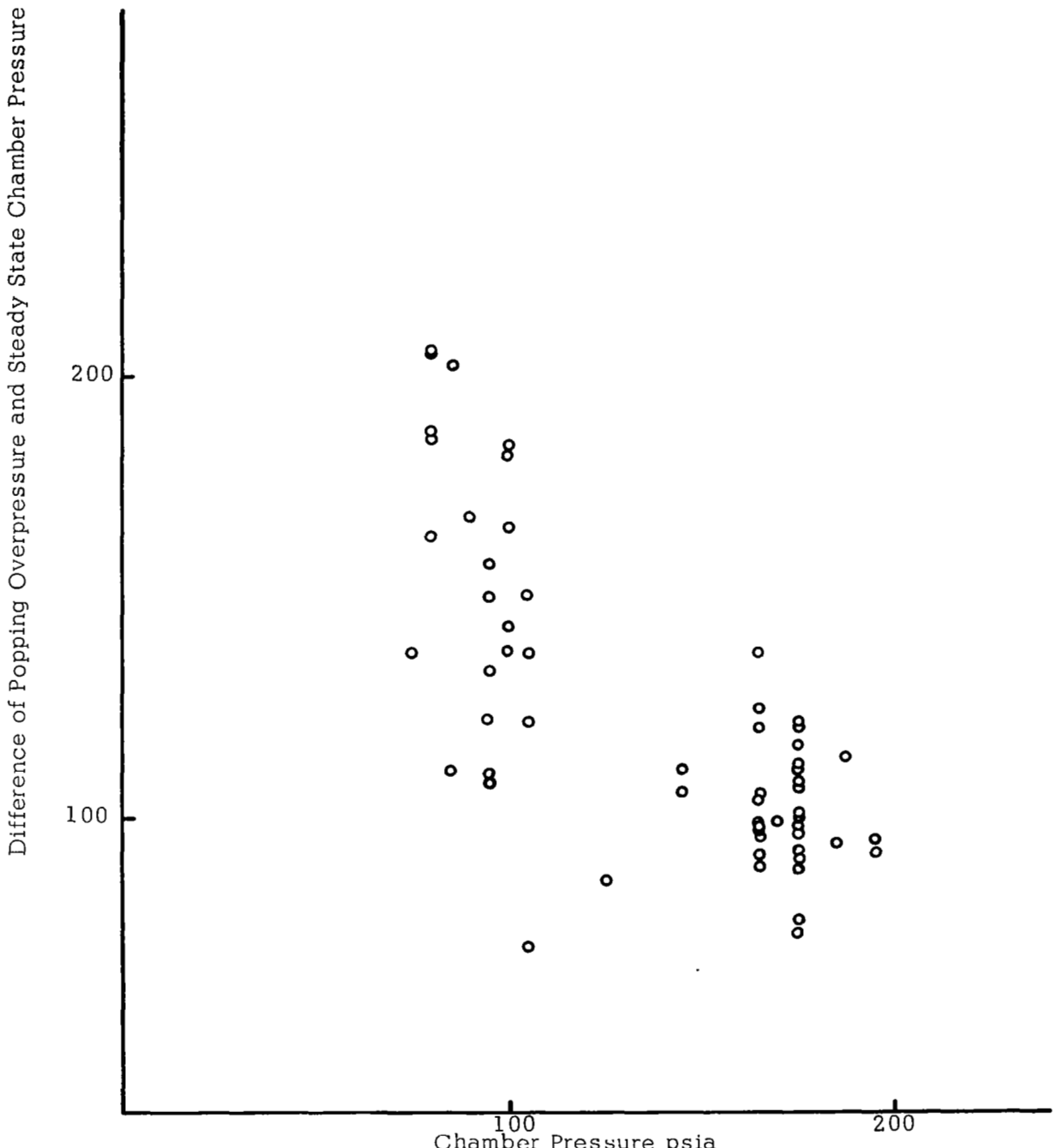

Figure 18. Variation of Popping Overpressure for Different Chamber Pressures.

RESULTS AND CONCLUSIONS

Both single exposure photography and high speed motion pictures were used to study three different combustion phenomena associated with impinging hypergolic propellant streams: combustor pressure poppings, stream mixing, and stream separation.

High speed motion pictures showed that popping is a violent explosion of the liquid propellant sprays. Chamber pressures were also recorded and were correlated with the photographically observed explosions. Pressure spikes of several hundred Psia were often observed resulting from these explosions. The occurrence of popping was found to depend significantly on chamber pressure and injector diameters. Using .055" and .060" injectors, experimental data showed that popping was almost absent for chamber pressures above 185 Psia, and was found to occur very frequently at lower chamber pressures. Popping was never observed using the smaller .027" orifice, and was observed only infrequently at low chamber pressures when .040" orifice was used. Popping frequency and average pressure spikes were obtained from the oscillograph data. Both the popping frequency and the magnitude of the pressure spikes are higher at lower chamber pressures. To summarize, the test results showed that popping was more likely to occur for larger orifice diameters at lower chamber pressures and steady state chamber operations were observed for smaller orifices at higher operating chamber pressures.

Stream mixing and separated flows were studied under steady state chamber operation conditions. Two distinctly different separated flows were observed. At low chamber pressures and for nitrogen tetroxide temperatures above the boiling point, vaporization of the oxidizer was significant, resulting in a gas/liquid impingement. The resulting spray pattern showed that hydrazine droplets were mainly confined on the fuel side. Photographs of the flame also showed that combustion mainly occurred on the fuel side indicating a separated flow. Separated flows were also observed with liquid/liquid impingement at higher chamber pressures (above 230 Psia). The resulting liquid sprays definitely showed color variations with colorless hydrazine along the fuel side of the spray and brownish liquid nitrogen tetroxide on the oxide side. This indicated very poor intermixing of droplets and ligaments of two liquid propellants. Stream mixing flows were observed at lower chamber pressures (less than 230 Psia) and with nitrogen tetroxide temperatures below the boiling point. The sprays resulting from liquid/liquid impingement showed a very uniform brownish color, indicating good intermixing of droplets and ligaments of the two propellants. To summarize, the test results showed that chamber pressure played a very significant role. Separated flows were observed at high chamber pressures and mixed flows were observed at lower chamber pressures. In addition, nitrogen tetroxide temperature was also found to be important. For nitrogen tetroxide temperature above the boiling point, gas/liquid impingement was observed resulting in separated flows.

REFERENCES

1. Rupe, J. H. "The Application of Nonreactive-Spray Properties to Rocket-Motor Injector Design," Tech. Rpt. 32-255, Jet Propulsion Laboratory, Pasadena, Calif. (July 15 1965).

2. Elverum, G. W. and Standhammer, P. "The Effect of Rapid Liquid Phase Reactions on Injector Design and Combustion in Rocket Motors." Progress Rpt. 30-4, Jet Propulsion Laboratory, Pasadena, Calif. (Aug 25, 1959).

3. Johnson, B. H., "An Experimental Investigation of the Effects of Combustion on the Mixing of Highly Reactive Liquid Propellants," Tech.Rept. 32-609. Jet Propulsion Laboratory, Pasadena, Calif. (July 15, 1965).

4. Evans, D. D., Stanford, H. B., and Riebling, R. W., "The Effect of Injector Element Scale on the Mixing and Combustion of Nitrogen Tetroxide-Hydrazine Propellant," Tech. Rept. 32-1178, Jet Propulsion Laboratory, Pasadena, Calif. (Nov. 1, 1967).

5. Burrows, M. C., "Mixing and Reaction Studies of Hydrazine and Nitrogen Tetroxide Using Photographic and Spectral Technique, AIAA Paper No. 67-107, AIAA 5th Aerospace Science Meeting, New York, (Jan. 1967).

6. Lawver, B. R. and Breen, B. P., "Hypergolic Stream Impingement Phenomena - Nitrogen Tetroxide/Hydrazine," NASA-CR-72444, Dynamic Science, Irvine, Calif. (Oct. 1968).

7. Breen, B. P., Zung, L. B., Lawver, B. R., Kosvic, T. C., and Coates, D. E., "Injection and Combustion of Hypergolic Propellants," AFRPL-TR-69-48, Dynamic Science, Irvine, Calif. (April 1969).

8. Campbell, D. T., Cline, G. L., Cordill, J. D., Proffit, R. L., and Sloat, T. N., "Reactive Stream Separation Photography," Interim Rept. Rocketdyne, division of North American Rockwell, Canoga Park, Calif. (Jan 10, 1970).

9. Lawver, B. R., "Rocket Engine Pop Design Criteria, " TCER 9642:0106, Aerojet General Corporation, Sacramento, Calif. (Sept. 1969).

10. Houseman, John, "Optimum Mixing of Hypergolic Propellants in an Unlike Doublet Injector Element," 6th ICRPG Combustion Conference, Vol. 1, CPIA Publication No. 192, December 1969, pp13-19

11. Kushida, R., and Houseman, J., "Criteria for Separation of Impinging Streams of Hypergolic Propellants," JPL Report WSCI-67-38, 1967.

APPENDIX A

NOMENCLATURE FOR TABULAR TEST DATA

F	=	Fuel
O	=	Oxidizer
W	=	Propellant Flow Rate (lb/sec)
T	=	Propellant Injection Temperature (^{o}F)
V	=	Propellant Injection Velocity (ft/sec)
M	=	Momentum of Propellant Stream (WV=16 ft/sec^{2})
$\bar{V}_a$	=	Average Injection Velocity = $(W_f V_f + W_o V_o)/W_o + W$)
$\frac{M_f}{M_o}$	=	Momentum Ratio of Fuel and Oxidizer Streams
D	=	Injector Orifice Diameter (equal fuel and oxidizer orifices)
$\bar{T}_a$	=	Average Injection Temperature=$(W_f T_f + W_o T_o)/W_f + W_o$)
$D/\bar{V}_a$	=	Ratio of Orifice Diameter to Average Injection Velocity
P	=	Chamber Pressure.

Test No.		W	T	V	M	$\bar{V}_a$	O/F	M_f/M_o	D	$\bar{T}_a$	$D/\bar{V}_a$	P	Comments
15	F	.0087	70	15.06	.1305	29.17	.942	1.621	.027	70	7.71×10^{-5}	14.7	Ox boiling; orifice out of alignment
	O	.0082	70	22.94	.188								
28	F	.0156	70	74.97	1.3945	60.68	.838	2.048	.027	70	4.45×10^{-5}	14.7	Ox boiling, orifice out of alignment.
	O	.0156	70	43.65	.6809								
58	F	.011	70	45.9	.505	51.7	1.78	.469	.027	68.7	4.3×10^{-5}		Poor flow, Ox rich appeared mixed.
	O	.0196	68	54.9	1.076								
61	F	.010	70	40.34	.4034	41.3	1.50	.641	.027	70	5.4×10^{-5}	14.7	Separated flow due to Ox boiling.
	O	.015	70	42.02	.63								
62	F	.0076	72	-	.234	37.6	1.95	.384	.027	72	5.9×10^{-5}	14.7	Separated flow due to Ox boiling.
	O												
63	F	.0128	70	51.55	.66	45.87	1.14	1.10	.027	68.3	4.9×10^{-5}	14.7	Mixed flow
	O	.0146	67	40.90	.597								
64	F	.0132	68	53.23	.729	49.5	1.21	1.016	.027	66.2	4.5×10^{-5}		Mixed flow
	O	.0160	65	44.83	.717								
68	F	.0195	70	78.45	1.53	74.0	1.29	.86	.027	70	3.04×10^{-5}	14.7	Separated flow due to Ox boiling
	O	.0252	70	70.60	1.78								
79	F	.0062	70	25.21	.78	22.23	1.11	1.162	.027	70	1.01×10^{-4}	14.7	Separated flow due to Ox boiling.
	O	.0069	70	19.55	.13								
80	F	.0134	68	54.35	.728	47.	1.09	1.220	.027	68	4.78×10^{-5}	14.7	Mixed flow.
	O	.0146	68	40.90	.597								
81	F	.0132	70	53.23	.704	43.8	.909	1.747	.027	70	5.13×10^{-5}	14.7	Separated flow due to Ox boiling.
	O	.0120	70	33.62	.403								
82	F	.0133	70	52.0	.682	46.1	.02	1.696	.027	70	4.88×10^{-5}	14.7	Separated flow due to Ox boiling.
	O	.0136	70	39.5	.402								
83	F		70	52.0	.692	46.1	1.079	1.195	.027	70	4.88×10^{-5}	14.7	Separated flow due to Ox boiling.
	O		70	40.5	.579								
85	F	.0118	70	47.6	.562	42.8	1.02	1.08	.027	70	5.25×10^{-5}	14.7	Separated flow due to boiling.
	O	.0136	70	38.1	.519								
89	F	.0060	68	24.4	.1475	21.5	1.10	1.18	.027	67.4	1.045×10^{-4}	14.7	Mixed flow
	O	.0067	67	18.6	.125								
90	F	.0233	67	94.3	2.197	72	.815	2.177	.027	67	3.2×10^{-5}	14.7	Mixed Flow
	O	.0190	67	53.2	1.011								
91	F	.0233	70	94.3	2.20	73.8	.815	2.177	"	70	3.05×10^{-5}	14.7	Separated flow due to Ox boiling
	O	.0190	70	53.2	1.01								
92	F	.0233	70	92	.208	78	1.02	1.38	"	70	2.89×10^{-5}	"	Separated flow due to Ox boiling
	O	.0190	70	65	.151								
93	F	.0147	60	59.6	.875	51.26	1.04	1.31	"	60	4.39×10^{-5}	"	Mixed flow
	O	.0154	60	43.4	.668								
94	F	.0139	45	56.0	.778	63.23	1.31	.83	"	45	4.75×10^{-5}	"	Mixed flow
	O	.0138	45	38.9	.537								
95	F	.0164	45	66.5	1.09	63.23	1.31	.83	"	45	3.62×10^{-5}	"	Mixed flow
	O	.0216	45	60.8	1.313								
96	F	.0072	45	29.3	.211	25.5	1.08	1.23	"	45	8.82×10^{-5}	"	Mixed flow rate too low
97	O	.0078	45	22.0	.172								Poor photography
98	F	.0072	45	29.3	.2109	25.72	1.11	1.17	"	45	8.75×10^{-5}	"	Mixed flow
	O	.0080	45	22.5	.180								
99	F	.0158	80	64.3	1.016	52.84	.89	1.80	"	80	4.26×10^{-5}	"	Separated flow due to Ox boiling
	O	.0141	80	40.0	.564								
100	F	.0082	80	33.0	.2706	26.88	.84	2.20	"	78	8.37×10^{-5}	"	Separated flow due to Ox boiling
	O	.0069	75	19.61	.1353								
101	F	.0089	83	36.14	.3216	28.92	.80	2.28	"	80	7.78×10^{-5}	"	Separated flow due to Ox boiling
	O	.0071	79	19.98	.1412								

Test No.		W	T	V	M	$\bar{V}_a$	O/F	M_f/M_o	D	$\bar{T}_a$	$D/\bar{V}_a$	P	Comments
102	F	.0059	82	24.09	.1421	21.01	1.10	1.20	"	80	0.71×10^{-5}	"	Time exposure photo
	O	.0065	78	18.21	.1184								
108	F	.0088	95	35.86	.3156	42.83	1.89	.407	.027	82.5	5.75×10^{-5}	14.7	Separated flow due to Ox boiling
	O	.0167	70	46.50	.776								
109	F	.0075	95	30.25	.2269	38.11	2.01	.405	"	82.5	5.91×10^{-5}	"	Separated flow due to Ox boiling
	O	.0151	70	42.02	.6345								
110	F	.0077	95	31.37	.2415	28.1	1.18	1.06	"	82.5	8.0×10^{-5}	"	Separated flow due to Ox boiling
	O	.0091	70	25.3	.2292								
111	F	.0059	65	23.6	.138	22.96	1.38	.76	"	65	9.8×10^{-5}	"	Mixed flow
	O	.0081	65	22.5	.1811								
112	F	.0082	65	33.2	.272	30	1.16	1.07	"	65	7.5×10^{-5}	"	Mixed flow
	O	.0096	65	26.7	.255								
113	F	.0082	110	33.2	.272	29	1.04	1.331	"	90	7.76×10^{-5}	"	Separated flow due to Ox boiling
	O	.0086	70	23.9	.2043								
114	F	.0067	105	27.17	.1820	22.65	.955	1.587	"	87.4	9.9×10^{-5}	"	Separated flow due to Ox boiling
	O	.0064	70	17.93	.1147								
116	F	.0067	105	22.17	.1820	27.05	.955	1.58	"	87.4	9.97×10^{-5}	"	Time exposure photo
	O	.0064	70	17.93	.1147								
117	F	.0061	80	24.8	.151	21.5	.96	1.58	"	75	1.04×10^{-4}	"	Time exposure photo
	O	.0059	70	16.3	.095								
118	F	.0172	80	69.5	1.195	60.17	1.07	1.28	.060	75	3.74×10^{-5}	"	Time exposure photo
	O	.0185	70	51.5	.953								
119	F	.0042	80	16.8	.07	15.41	1.23	.95	"	75	14.6×10^{-5}	"	Separated flow due to Ox boiling
	O	.0052	70	14.3	.074								
120	F	.0046	80	21.8	.0998	19.18	1.12	1.15	"	75	11.73×10^{-5}	"	Time exposure photo
	O	.0051	70	16.85	.0866								
121	F	.0118	80	47.9	.565	41.70	1.09	1.21	.060	75	5.39×10^{-5}	14.7	Time exposure photo
	O	.0129	70	36.1	.465								
122	F	.0227	80	92.5	2.1	79.74	1.06	1.28	"	75	2.82×10^{-5}	"	Time exposure photo
	O	.0242	70	67.6	1.64								
123	F	.0216	75	18.1	.39	15.39	1.16	1.06	"	75	1.39×10^{-5}	"	Separated flow due to Ox boiling
	O	.0251	75	13.19	.349								
124	F	.0158	72	12.51	.197	10.45	.95	1.06	"	71.5	4.784×10^{-5}	"	Separated flow due to Ox boiling
	O	.0150	71	8.34	.125								
125	F	.0135	72	10.65	.144	8.77	.89	1.81	"	71.4	5.70×10^{-4}	"	Separated flow due to Ox boiling
	O	.0120	71	6.64	.0797								
126	F	.0108	72	8.56	.092	7.02	.90	1.77	"	72	7.12×10^{-4}	"	Separated flow due to Ox boiling
	O	.0097	72	5.38	.052								
127	F	.0071	72	5.60	.0397	4.94	1.10	1.17	"	72	1.0×10^{-3}	"	Separated flow due to Ox boiling
	O	.0078	72	4.34	.0339								
128	F	.0208	50	16.46	.342	14.54	1.11	1.15	"	54	3.44×10^{-4}	"	Popping
	O	.0232	40	12.84	.298								
129	F	.0172	52	13.61	.234	11.39	.96	1.56	"	56.8	4.39×10^{-4}	"	Popping
	O	.0165	42	9.13	.150								
130	F	.0130	52	10.26	.133	9.33	1.18	1.01	"	56.4	5.36×10^{-4}	"	Popping
	O	.0154	42	8.56	.132								
131	F	.0113	52	8.95	.101	8.40	1.27	.88	"	56.8	5.95×10^{-4}	"	Popping
	O	.0144	42	8.01	.115								
132	F	.0100	52	7.90	.079	9.35	1.83	.425	"	56.8	5.35×10^{-4}	"	Popping
	O	.0103	45	10.15	.1857								

Test No.		W	T	V	M	$\bar{V}_a$	O/F	M_f/M_o	D	$\bar{T}_a$	$D/\bar{V}_a$	P	Comments
133	F	.0150	50	11.85	.177	10.76	1.18	1.0	"	54.5	4.65×10^{-4}	"	Popping
	O	.0178	45	9.88	.176								
134	F	.0168	50	13.28	.223	11.30	1.0	1.423	.060	53.8	4.43×10^{-4}	14.7	Popping
	O	.0168	47	9.33	.1567								
135	F	.0108	62	8.56	.0924	6.77	.71	2.81	"	52.2	7.39×10^{-4}	"	Popping
	O	.0077	63	4.28	.0329								
136	F	.0183	54	14.49	.265	13.05	1.17	1.047	"	61.8	3.83×10^{-3}	"	Popping
	O	.0214	54	11.85	.253								
137	F	.0153	55	12.13	.185	10.17	1.04	1.54	"	54.8	4.92×10^{-4}	"	Popping
	O	.0147	55	8.18	.1202								
139	F	.0153	61	12.07	.185	10.77	1.13	1.11	"	60.8	4.64×10^{-4}	"	Popping
	O	.0173	61	9.60	.166								
140	F	.0253	63	19.98	.505	16.81	.98	1.47	"	62.8	2.97×10^{-4}	"	Popping
	O	.0249	63	13.83	.344								
141	F	.0139	70	25.53	.355	23.37	1.20	.986	.040	68	1.43×10^{-4}	"	Popping
	O	.0167	66	21.57	.360								
142	F	.0113	70	20.81	.235	19.20	1.22	.951	"	69.8	1.74×10^{-4}	"	Separated flow due to Ox boiling
	O	.0138	70	17.87	.247								
143	F	.0094	70	17.23	.161	14.96	1.07	1.25	"	69.8	2.23×10^{-4}	"	Separated flow due to Ox boiling
	O	.010	70	12.89	.129								
144	F	.0076	70	14.04	.107	12.71	1.18	1.03	"	69.8	2.62×10^{-4}	"	Separated flow due to Ox boiling
	O	.0090	70	11.62	.104								
148	F	.0094	92	17.23	.162	19.47	1.71	.488	"	81.9	1.71×10^{-4}	"	Separated flow due to Ox boiling
	O	.0160	72	20.68	.331								
149	F	.0151	68	27.8	.420	25.51	1.21	.97	.040	68	1.31×10^{-4}	14.7	Mixed
	O	.0183	68	23.62	.432								
150	F	.0154	59	28.34	.437	25.97	1.20	.98	"	63.8	1.28×10^{-4}	"	Popping
	O	.0186	67	24.00	.446								
151	F	.0104	65	19.15	.268	20.56	1.22	1.29	"	63.1	1.62×10^{-4}	"	Popping
	O	.0127	61.5	16.34	.207								
152	F	.0104	63	19.15	.199	16.31	1.01	1.40	"	62.8	2.04×10^{-4}	"	Mixed
	O	.0105	62.5	13.53	.142								
164	F	.0119	73	21.95	.2612	19.07	1.068	1.25	"	71.6	1.75×10^{-4}	149	Mixed flow
	O	.0127	68.5	16.39	.2081								
165	F	.0126	73	23.23	.2927	23.38	1.44	.685	"	69.2	1.43×10^{-4}	189	Mixed flow
	O	.0182	67	23.49	.4275								
166	F	.0126	73	23.23	.2927	23.76	1.47	.652	"	69.7	1.40×10^{-4}	187	Mixed flow
	O	.0186	66	24.12	.4486								
167	F	.0135	59	24.76	.3343	23.88	1.35	.79	"	51.9	1.39×10^{-4}	189	Mixed flow
	O	.0182	47	23.23	.4228								
169	F	.0144	51.5	26.55	.3823	25.17	1.31	.838	"	44.7	1.324×10^{-4}	209	Difficult to define
	O	.0189	40	24.13	.4560								
170	F	.0082	57.5	15.06	.1235	15.13	1.45	.683	"	46.7	2.203×10^{-4}	111	Mixed flow
	O	.0119	40.	15.19	.1807								
171	F	.0144	58	26.55	.3823	24.58	1.25	.923	"	49.2	1.356×10^{-4}	191	Mixed flow
	O	.0180	42.5	23.0	.4140								
174	F	.0145	64	26.55	.3850	24.25	1.20	.99	.040	58.2	1.374×10^{-4}	172	Mixed flow
	O	.0174	53.7	22.34	.3887								
175	F	.0145	65	26.55	.3850	24.25	1.20	.99	"	60.4	1.374×10^{-4}	187	Mixed flow
	O	.0174	57	22.34	.3887								
179	F	.0126	62.5	23.23	.2926	22.07	1.30	.842	"	58.6	1.51×10^{-4}	163	Mixed flow
	O	.0164	56	21.19	.3475								

Test No.		W	T	V	M	$\bar{V}_a$	O/F	M_f/M_o	D	$\bar{T}_a$	$D/\bar{V}_a$	P	Comments
180	F	.0129	80.5	23.74	.3062	21.07	1.55	1.07	"	77.9	1.57×10^{-4}	165	Mixed flow
	O	.0149	76	19.14	.2852								
181	F	.0111	81.5	20.42	.2267	18.86	1.234	.94	"	78.3	1.77×10^{-4}	140	Mixed flow
	O	.0137	76.5	17.61	.2412								
182	F	.0106	87	19.40	.2049	19.67	1.47	.66	"	82	1.70×10^{-4}	259	Difficult to define
	O	.0155	80.5	19.91	.3086								
183	F	.0158	93	29.10	.4598	24.27	.943	1.61	"	88.7	1.37×10^{-4}	157	Mixed flow
	O	.0149	84.5	19.15	.2853								
184	F	.0074	100.5	13.53	.0997	15.85	1.83	.425	"	96.7	2.10×10^{-4}	119	Mixed flow
	O	.0135	95	17.36	.2344								
185	F	.0096	95.5	17.62	.1691	17.42	1.41	.721	"	102.7	1.91×10^{-4}	131	Mixed flow
	O	.0135	106.5	17.36	.2344								
186	F	.0129	91	23.74	.3069	22.58	1.31	.837	.040	82.6	1.48×10^{-4}	155	Mixed flow
	O	.0169	76.5	21.70	.3667								
187	F	.0147	90.5	27.06	.3978	26.76	1.41	.723	"	90	1.25×10^{-4}	194	Mixed flow
	O	.0207	90.5	26.55	.5496								
188	F	.0160	90	29.36	.4698	27.46	1.24	.92	"	87.3	1.22×10^{-4}	194	Mixed flow
	O	.0199	85.5	25.53	.5080								
191	F	.0136	102.5	25.02	.3408	24.88	1.42	.713	"	98.8	1.34×10^{-4}	170	Mixed flow
	O	.0193	96	24.76	.4778								
192	F	.0147	113	27.06	.3978	25.35	1.27	.886	"	107.5	1.32×10^{-4}	152	Mixed flow
	O	.0187	103.5	24.00	.4488								
193	F	.0167	99	30.76	.5137	27.42	1.14	1.097	"	95.9	1.22×10^{-4}	174	Mixed flow
	O	.0191	93.5	24.51	.4681								
194	F	.0164	104	30.12	.4939	26.74	1.13	1.12	"	101.7	1.25×10^{-4}	169	Mixed flow
	O	.0185	100	23.74	.4392								
196	F	.0172	94	31.66	.5445	27.67	1.09	1.21	"	88	1.204×10^{-4}	194	Mixed flow
	O	.0187	75.5	24.00	.4488								
197	F	.0172	75.5	31.66	.5445	25.05	.72	2.79	"	87.4	1.331×10^{-4}	187	Mixed flow
	O	.0123	105.5	15.83	.1947								
198	F	.0147	100.5	27.06	.3978	25.14	1.25	.92	"	94.7	1.33×10^{-4}	164	Mixed flow
	O	.0184	90.5	23.61	.4344								
199	F	.0176	108	32.42	.570	27.73	1.03	1.36	"	100	1.20×10^{-4}	181	Mixed flow
	O	.0181	92.5	23.23	.420								
200	F	.0172	77	31.66	.5445	27.23	1.04	1.324	.040	70	1.224×10^{-4}	203	Appeared to be mixed flow
	O	.0179	64	22.98	.4113								
201	F	.0172	77	31.66	.5445	26.25	.924	1.68	"	69.6	1.27×10^{-4}	178	Mixed flow
	O	.0159	62	20.42	.3247								
204	F	.0194	63.5	35.74	.693	32.92	1.23	.95	"	56.7	1.01×10^{-4}	110	Mixed flow
	O	.0238	51.5	30.64	.729								
205	F	.0189	84	34.72	.656	33.83	1.36	1.36	"	79.2	9.85×10^{-5}	115	Mixed flow
	O	.0257	76	33.19	.853								
206	F	.0163	94.5	29.87	.4869	32.06	1.59	1.59	"	91.8	1.04×10^{-4}	115	Mixed flow
	O	.0259	90.5	33.44	.8661								
207	F	.0183	106.5	33.70	.6167	31.16	1.23	1.23	"	108	1.069×10^{-4}	110	Mixed flow
	O	.0226	109.5	29.10	.6577								
208	F	.0217	108	39.83	.8643	33.86	.99	1.44	"	104.6	9.8×10^{-5}	110	Mixed flow
	O	.0215	101.5	27.83	.5983								
209	F	.0189	110	34.72	.6562	31.66	1.19	.99	"	106.8	1.05×10^{-5}	110	Mixed flow
	O	.0226	104.5	29.10	.6577								
210	F	.0201	110	37.02	.7441	32.83	1.12	1.13	"	115.6	1.02×10^{-4}	110	Mixed flow
	O	.0226	121	29.10	.6577								

Test No.		W	T	V	M	$\bar{V}_a$	O/F	M_f/M_o	D	$\bar{T}_a$	$D/\bar{V}_a$	P	Comments
211	F	.0189	116	34.72	.6562	32.17	1.24	.93	"	118.0	1.04×10^{-4}	110	Mixed flow
	O	.0234	121	30.12	.7048								
212	F	.0189	117.5	34.72	.6562	32.18	1.24	.93	"	119.2	1.04×10^{-4}	110	Mixed flow
	O	.0234	121	30.13	.705								
215	F	.0368	118	67.66	2.490	61.17	1.17	.852	.040	112.4	5.45×10^{-5}	110	Mixed flow
	O	.0432	108	55.66	2.404								
217	F	.0368	101	67.66	2.490	61.17	1.17	.852	"	96.5	5.45×10^{-5}	110	Mixed flow
	O	.0432	93	55.6b	2.404								
219	F	.0345	120.7	63.32	2.184	59.45	1.27	.787	"	122	5.61×10^{-5}	110	Mixed flow
	O	.0438	123.4	56.42	2.471								
220	F	.0368	122	67.66	2.490	60.20	1.13	.88	"	118.9	5.54×10^{-5}	110	Mixed flow
	O	.0416	116.5	53.61	2.230								
221	F	.0368	110	67.66	2.490	62.72	1.24	.808	"	105.9	5.32×10^{-5}	110	Mixed flow
	O	.0455	103	58.72	2.672								
222	F	.0368	114.4	67.66	2.490	60.80	1.16	.86	"	116.4	5.48×10^{-5}	110	Mixed flow
	O	.0426	118.5	54.89	2.338								
223	F	.0368	114.4	67.66	2.490	63.11	1.52	.798	"	116.5	5.28×10^{-5}	110	Photograph of plume
	O	.0461	118.5	59.49	2.742								
231	F	.0361	66.5	66.38	2.396	58.36	1.1	1.18	.040	72.6	5.71×10^{-5}	350	Separated flow
	O	.0396	78.5	51.06	2.022								
232	F	.0361	71.5	66.38	2.396	60.15	1.18	1.00	"	78.6	5.54×10^{-5}	380	Separated flow
	O	.0426	85	54.89	2.338								
234	F	.0368	117.5	67.66	2.49	68.07	1.12	.883	"	117.3	4.897×10^{-5}	353	Separated flow
	O	.0412	117.5	68.42	2.82								
235	F	.0368	102.5	67.66	2.49	58.61	1.05	.948	"	93.8	5.68×10^{-5}	353	Separated flow
	O	.0388	84	50.04	1.941								
236	F	.0340	89.5	62.55	2.127	54.72	1.08	.924	"	79.4	6.09×10^{-5}	346	Separated flow
	O	.0368	70.5	47.48	1.747								
237	F	.0368	93.2	67.66	2.490	61.44	1.18	.844	"	67.5	5.43×10^{-5}	362	Separated flow
	O	.0436	63	56.17	2.450								
239	F	.0368	85	67.66	2.490	58.61	1.05	.95	"	74.8	5.7×10^{-5}	361	Separated flow
	O	.0388	65.5	50.04	1.941								
239	F	.0146	82	26.80	.3912	24.44	1.19	1.0	"	76.4	1.36×10^{-4}	145	Mixed
	O	.0174	72	22.47	.3909								
240	F	.0368	66.5	67.66	2.490	66.17	1.37	.76	"	64.3	5.04×10^{-5}	238	Undefined
	O	.0505	63	65.10	3.287								
241	F	.0368	117	67.66	4.250	71.55	1.56	.586	"	115.3	4.66×10^{-5}	230	Mixed flow
	O	.0574	114.5	74.04	2.585								
242	F	.0375	126.5	68.93	2.585	61.46	1.14	1.11	"	136.8	5.42×10^{-5}	176	Mixed flow
	O	.0426	146.2	54.89	2.338								
243	F	.0375	122	68.93	2.585	61.47	1.135	1.11	"	119	5.42×10^{-5}	176	Mixed flow
	O	.0425	117	54.89	2.337								
244	F	.0352	53.5	64.59	2.273	52.85	.866	1.89	.040	52	6.31×10^{-5}	338	Separated flow
	O	.0305	44.2	39.32	1.199								
246	F	.0334	40.6	61.27	2.046	58.65	1.31	.822	"	39.9	5.68×10^{-5}	400	Separated flow
	O	.0439	39.4	56.68	2.488								
247	F	.0360	61.5	66.12	2.380	61.58	1.25	.915	"	55.3	5.41×10^{-5}	215	Mixed flow
	O	.0449	50.7	57.95	2.602								
248	F	.0354	60	65.10	2.304	62.89	1.34	.792	"	55.4	5.3×10^{-5}	115	Mixed flow
	O	.0475	50.5	61.27	2.910								
250	F	.0368	69.5	67.66	2.490	64.06	1.29	.885	"	62.8	5.20×10^{-5}	218	Mixed
	O	.0475	58	61.27	2.910								

Test No.		W	T	V	M	$\bar{V}_a$	O/F	M_f/M_o	D	$\bar{T}_a$	$D/\bar{V}_a$	P	Comments
251	F	.0354	73.5	65.10	2.304	60.16	1.23	.94	"	66.7	5.54×10^{-5}	384	Separated
	O	.0436	61.5	56.17	2.449								
252	F	.0272	75.5	50.04	1.361	47.16	1.28	.871	"	69.4	7.07×10^{-5}	307	Not defined
	O	.0348	65	44.93	1.563								
253	F	.0208	77	38.30	.7966	36.28	1.29	.853	"	71.4	9.19×10^{-5}	507	Separated
	O	.0269	67.5	34.72	.9339								
254	F	.0208	85.5	28.30	.5886	32.55	1.33	.594	"	80.4	1.02×10^{-4}	520	Separated
	O	.0277	77	35.74	.99								
255	F	.0285	103	52.34	1.492	50.16	1.32	.818	"	105	6.65×10^{-5}	84	Mixed
	O	.0376	105.5	48.51	1.824								
256	F	.0354	119.5	65.10	2.304	60.11	1.26	.917	"	123	5.55×10^{-5}	99.6	Mixed
	O	.0447	126	56.17	2.511								
257	F	.0361	120	66.38	2.396	60.79	1.20	.981	.040	121.9	5.48×10^{-5}	99.6	Mixed
	O	.0435	123.5	56.17	2.443								
258	F	.0200	104	36.76	.7352	33.95	1.22	.95	"	97.7	9.82×10^{-5}	422.7	Separated
	O	.0245	93	31.66	.7757								
259	F	.0203	99	37.27	.756	34.45	1.22	.843	"	96.3	9.68×10^{-5}	461	Separated
	O	.0249	93.5	32.17	.801								
260	F	.0200	84	36.76	.723	33.80	1.24	.917	"	98.3	9.86×10^{-5}	461	Separated
	O	.0247	74	31.91	.788								
261	F	.0200	88	36.76	.735	33.43	1.18	1.01	"	92.9	9.97×10^{-5}	115	Mixed
	O	.0237	79	30.64	.726								
262	F	.0225	96.5	41.36	.9306	37.37	1.18	1.04	"	93.9	8.92×10^{-5}	130	Mixed
	O	.0263	92	33.96	.8931								
263	F	.0285	96.5	52.34	1.491	46.05	1.1	1.18	"	92.6	7.24×10^{-5}	149	Mixed
	O	.0313	89.5	40.34	1.263								
264	F	.0288	96.5	52.98	1.526	49.10	1.24	.933	"	92.6	6.80×10^{-5}	169	Mixed
	O	.0356	89.5	45.95	1.636								
265	F	.0334	92.5	61.27	2.046	55.41	1.17	1.03	"	87.7	6.01×10^{-5}	188	Mixed
	O	.0392	84	50.55	1.981								
266	F	.0375	92.5	68.93	2.585	62.07	1.16	.862	"	87.2	5.37×10^{-5}	203	Mixed
	O	.0435	83	56.17	2.443								
267	F	.0368	88	67.65	2.489	62.44	1.22	.948	"	83.7	5.34×10^{-5}	388	Separated
	O	.0451	80.5	58.21	2.625								
268	F	.0312	86	57.44	1.792	57.88	1.44	.683	"	80.8	5.76×10^{-5}	381	Separated
	O	.0451	77.5	58.21	2.625								
269	F	.0285	86	52.34	1.492	53.87	1.49	.669	"	80.4	6.19×10^{-5}	353	Separated
	O	.0426	77	54.89	2.330								
270	F	.0389	129	71.48	2.781	60.27	.966	1.52	.040	134.6	5.531×10^{-5}	176	Mixed flow
	O	.0376	137.6	48.51	1.824								
272	F	.0341	111	62.55	2.133	59.1	1.28	.865	"	107.7	5.64×10^{-5}	179	Mixed flow
	O	.0437	105.5	56.42	2.465								
273	F	.0341	123.5	62.55	3.133	59.94	1.31	.82	"	121.4	5.56×10^{-5}	176	Mixed flow
	O	.0449	120.	57.95	2.602								
274	F	.0250	120	45.95	1.149	51.58	1.7	.49	"	117.9	6.46×10^{-5}	176	Mixed flow
	O	.0426	117	54.89	2.338								
275	F	.0278	117	51.06	1.419	46.21	1.17	1.03	"	114.9	7.21×10^{-5}	138	Mixed flow
	O	.0327	113.5	42.3	1.377								
276	F	.040	70.	73.4	2.936	74.11	1.447	.679	"	70	4.49×10^{-5}	279	Flow undefined
	O	.0579	70.	74.7	4.32								
278	F	.0397	70	73.4	2.91	66.47	1.187	.983	"	70	5.0×10^{-5}	237	Mixed flow
	O	.0471	70	60.76	2.86								

Test No.		W	T	V	M	$\bar{V}_g$	O/F	M_f/M_o	D	$\bar{T}_a$	$D/\bar{V}_a$	P	Comments
279	F	.0297	70	73.4	7.914	69.27	1.292	1.16	"	70	4.81×10^{-5}	250	Mixed flow
	O	.0513	70	66.12	3.39								
281	F	.069	73.5	126.8	8.74	112.5	1.13	1.115	"	71	2.96×10^{-5}	100	Mixed flow
	O	.078	69	100.5	7.83								
282	F	.069	72.5	126.5	8.73	117.2	1.54	.872	"	70	2.66×10^{-5}	115	Mixed flow
	O	.091	67	117	10.05								
283	F	.053	97.5	97.5	5.16	97.7	1.22	.943	.040	60	3.8×10^{-5}	326	Separated flow
	O	.065	94.2	84.2	5.47								
284	F	.050	74	93.1	4.65	83.5	1.16	1.06	"	63	3.38×10^{-5}	282	Separated flow
	O	.058	54	73.5	4.37								
285	F	.042	86	77.8	3.26	69.7	1.16	1.06	"	69	4.78×10^{-5}	228	Mixed flow
	O	.049	54	62.8	3.08								
286	F	.034	86	62.8	2.13	55.5	1.14	1.06	"	69	5.9×10^{-5}	192	Mixed flow
	O	.039	54	51.3	2.00								
287	F	.027	86	51.06	1.37	46.8	1.25	.92	"	69	7.12×10^{-5}	182	Mixed flow
	O	.024	55	44.1	1.49								
288	F	.018	57	51.8	0.93	47.9	1.89	.597	"	60	6.94×10^{-5}	186	Mixed flow
	O	.034	62	45.9	1.56								
289	F	.028	55	53.2	1.48	50.5	1.32	.822	"	59	6.60×10^{-5}	174	Mixed flow
	O	.037	62	48.7	1.80								
290	F	.030	101	56.4	1.69	55.0	1.03	.782	"	98	6.06×10^{-5}	186	Mixed flow
	O	.040	95.5	54.1	2.16								
291	F	.029	71	54.3	1.57	48.3	1.13	1.09	"	89	6.9×10^{-5}	162	Mixed flow
	O	.033	105.5	43.6	1.43								
293	F	.065	62	121	7.86	105.7	1.09	1.20	.060	61	3.15×10^{-5}	362	High speed movies recording, separated
	O	.071	60	91.9	6.52								
294	F	.029	64	54.3	1.57	40.8	1.24	.94	"	62	6.69×10^{-5}	180	High speed movie recording, mixed
	O	.036	60	46.4	1.67								
295	F	.034	53	72.5	2.46	67.2	1.44	.78	"	57	4.96×10^{-5}	14.7	High speed movie recording,popping observed
	O	.049	59	63.8	3.12								
296	F	.033	54	60.7	2.03	54.7	1.15	1.09	.060	55	6.09×10^{-5}	14.7	High speed movie recording, popping observed
	O	.038	57	49.0	1.86								
297	F	.030	55	60.7	1.82	41.4	1.23	1.01	"	56	8.0×10^{-5}	68	High speed movie recording popping observed
	O	.037	57	48.5	1.79								
298	F	.029	41	53.4	1.54	49.2	1.20	0.96	.040	47	6.77×10^{-5}	76	High speed movie recording mixed flow
	O	.035	51.5	46.2	1.61								
299	F	.029	40	53.3	1.54	44.8	0.93	1.59	"	46	7.44×10^{-5}	106	High speed movie recording mixed flow
	O	.027	53	35.9	0.97								
300	F	.030	41	36.6	1.69	50.7	1.11	1.05	"	47	6.57×10^{-5}	122	High speed movie recording mixed flow
	O	.035	53	46.2	1.61								
301	F	.031	41	57.4	1.77	51.6	1.16	1.05	"	47	5.46×10^{-5}	100	High speed movie recording mixed flow
	O	.036	53	47.2	1.69								
302	F	.031	43	57.4	1.77	46.5	1.07	1.74	"	49	7.17×10^{-5}	192	High speed movie recording mixed flow
	O	.029	55	35.5	1.02								
304	F	.023	37	42.4	.98	35.5	1.04	1.41	"	37	9.4×10^{-5}	14.7	High speed movie recording popping observed
	O	.024	37	28.9	.69								
305	F	.01	42	16.2	.16	14.5	1.0	1.27	"	42	2.3×10^{-4}	"	High speed movie recording mixed flow
	O	.01	42.5	12.8	.13								
306	F	.01	44	16.2	.16	16.14	1.26	0.80	"	41	2.06×10^{-4}	"	High speed movie recording popping observed
	O	.01	38.5	16.1	.20								
307	F	.026	32	48.5	1.26	50.8	1.58	0.59	"	32	6.5×10^{-5}	"	High speed movie recording mixed flow
	O	.041	32	52.3	2.15								

Test No.		W	T	V	M	$\bar{V}_a$	O/F	M_f/M_o	D	$\bar{T}_a$	$D/\bar{V}_a$	P	Comments
308	F	.0296	58.5	54.9	1.65	53.2	1.3	.86	"	58	6.25×10^{-5}	"	Popping based on O-graph record
	O	.0388	58	49.5	1.92								
309	F	.035	58.5	66.4	2.22	59.1	1.25	.86	.040	58	5.63×10^{-5}	14.7	Popping based on O-graph record
	O	.045	58	57.5	2.59								
310	F	.037	77.5	67.5	3.04	68.7	1.25	1.17	"	73	4.85×10^{-5}	"	Mixed flow
	O	.045	69.5	57.5	2.59								
311	F	.037	66.	67.5	3.04	68.7	1.25	1.17	"	62	4.85×10^{-5}	"	Mixed flow
	O	.045	59.5	57.5	2.59								
312	F	.037	61	67.7	2.50	65.5	1.25	.80	"	65	5.0×10^{-5}	"	Mixed flow
	O	.049	66	63.8	3.13								
313	F	.037	55	67.7	2.50	65.5	1.25	.80	"	54	5.0×10^{-5}	"	Mixed flow
	O	.049	53	63.8	3.13								
314	F	.037	55	67.7	2.50	64.7	1.29	.80	"	54	5.1×10^{-5}	"	Mixed flow
	O	.048	53	62.6	3.00								
316	F	.034	51	62.6	2.13	62.5	1.44	.70	"	48	5.3×10^{-5}	"	Mixed flow
	O	.049	48	62.6	3.06								
317	F	.029	51	54.9	1.59	47.4	1.45	.71	"	48	7.0×10^{-5}	"	Popping based on O-graph record
	O	.042	45	53.6	2.25								
318	F	.015	51	28.1	.43	24.96	1.15	1.09	"	49	1.3×10^{-4}	"	Mixed flow
	O	.018	48	22.5	.40								
319	F	.015	51	28.1	.43	27.41	1.36	.768	"	48	1.2×10^{-4}	"	Mixed flow
	O	.021	45	26.8	.56								
320	F	.010	54.5	19.2	.19	18.5	1.40	.76	"	55	1.8×10^{-4}	"	Popping based on O-graph records
	O	.014	55	18.0	.25								
321	F	.010	58.5	19.3	.193	18.6	1.40	.758	"	57	1.8×10^{-4}	"	Popping based on O-graph records
	O	.014	56.5	18.1	.255								
322	F	.011	60.5	19.4	.213	18.97	1.29	.818	.040	60	1.75×10^{-4}	14.7	Mixed flow
	O	.014	58.	18.38	.261								
323	F	.010	51	19.4	.194	19.10	1.46	.703	"	53	1.74×10^{-4}	"	Popping based on O-graph record
	O	.015	49.5	18.9	.276								
324	F	.009	51	17.9	.161	18.28	1.57	.623	"	50	1.82×10^{-4}	"	Mixed flow
	O	.014	49.5	18.1	.259								
325	F	.03	71.5	24.0	.721	23.13	1.37	.782	"	69	2.2×10^{-5}	"	Mixed flow
	O	.041	62.5	22.5	.923								
326	F	.03	51	23.8	.715	22.58	1.30	.847	.060	55	2.2×10^{-4}	"	Popping based on O-graph record
	O	.039	57.5	21.6	.844								
327	F	.03	47.5	23.4	.692	22.27	1.30	.837	"	48	2.2×10^{-4}	"	Popping based on O-graph record
	O	.039	48.0	21.4	.827								
328	F	.030	54.5	23.8	.715	22.70	1.31	.83	"	50	2.2×10^{-4}	"	Popping based on O-graph record
	O	.039	46.5	21.9	.861								
329	F	.030	52.5	23.8	.704	22.2	1.27	.90	"	49	2.25×10^{-4}	"	Popping based on O-graph record
	O	.038	46.5	20.9	.784								
330	F	.030	52.5	23.8	.705	22.2	1.27	.90	"	50	2.25×10^{-4}	"	Popping based on O-graph record
	O	.038	47.5	20.9	.784								
331	F	.039	60.5	30.7	1.20	28.4	1.24	.92	"	62	1.75×10^{-4}	"	Popping based on O-graph record
	O	.049	64.0	26.9	1.31								
332	F	.055	64.0	43.4	2.38	38.3	1.11	1.16	"	63	1.3×10^{-4}	75	Popping based on O-graph record
	O	.061	63.0	33.8	2.06								
333	F	.063	64.0	49.8	3.44	44.4	1.13	1.12	"	63	1.1×10^{-4}	80	Popping based on O-graph record
	O	.071	63.0	39.6	2.81								
334	F	.073	63.0	57.4	4.20	46.6	.822	2.08	"	62	1.0×10^{-4}	95	Popping based on O-graph record
	O	.060	60.5	33.5	2.01								

Test No.		W	T	V	M	$\bar{V}_a$	O/F	M_f/M_o	D	$\bar{T}_a$	$D/\bar{V}_a$	P	Comments
335	F	.039	60.5	30.7	4.98	37.2	1.23	1.57	.060	62	1.3×10^{-4}	95.5	Popping based on O-graph record
	O	.048	64.0	26.4	1.26								
336	F	.055	64.0	43.6	2.39	38.5	1.11	1.15	"	64	1.2×10^{-4}	70	"
	O	.061	63.0	34.0	2.08								
337	F	.073	66.	57.4	4.19	47.4	.89	1.78	"	56	1.0×10^{-4}	80	"
	O	.065	61	36.2	2.35								
338	F	.063	89	49.7	3.13	45.9	1.24	.937	"	87	1.0×10^{-4}	85	"
	O	.078	86	43.0	3.34								
339	F	.074	96.5	57.8	4.28	51.1	1.11	1.16	"	100	9.7×10^{-5}	125	"
	O	.082	108	45.0	3.69								
340	F	.063	117	49.8	3.14	42.9	1.05	1.31	"	112	1.2×10^{-4}	75	"
	O	.066	108	36.3	2.40								
341	F	.063	107	50.1	3.16	45.1	1.16	1.06	"	103	1.1×10^{-4}	75	"
	O	.073	99.5	40.7	2.97								
342	F	.063	107	50.1	3.16	45.6	1.21	.994	"	102	1.0×10^{-4}	145	"
	O	.076	99	41.9	3.18								
343	F	.063	118	49.8	3.14	44.8	1.16	1.06	"	110	1.1×10^{-4}	145	"
	O	.073	103	40.5	2.96								
344	F	.063	81	49.8	3.14	49.9	1.24	.807	"	80	1.0×10^{-4}	145	"
	O	.078	79.5	43.3	3.89								
345	F	.062	81	49.1	3.04	45.9	1.26	.899	"	79	1.0×10^{-4}	165	"
	O	.078	77.5	43.3	3.38								
346	F	.063	75.5	49.8	3.14	46.2	1.28	.88	"	76	1.08×10^{-4}	165	"
	O	.080	76	44.5	3.56								
347	F	.063	79.5	48.8	3.14	46.5	1.25	.918	"	79	1.08×10^{-4}	165	"
	O	.079	78	43.54	3.42								
348	F	.063	83.3	49.8	3.14	41.3	.911	1.72	.060	83	1.21×10^{-4}	165	Popping based on motion picture & O-graph recording
	O	.057	82.5	31.8	1.83								
349	F	.064	91.0	50.5	3.23	42.1	.931	1.64	"	91	1.19×10^{-4}	"	"
	O	.060	89.5	33.0	1.97								
350	F	.064	91.0	50.5	3.23	44.8	1.12	1.13	"	92	1.12×10^{-4}	165	"
	O	.072	93.5	39.7	2.85								
351	F	.063	72.0	49.8	3.14	48.3	1.35	7.82	"	71	1.03×10^{-4}	"	"
	O	.085	69.5	47.2	4.02								
352	F	.062	71.5	49.1	3.04	44.8	1.21	.98	"	69	1.1×10^{-4}	165	Popping not observed
	O	.075	67.5	41.4	3.10								
353	F	.062	70	48.6	3.02	45.2	1.23	.938	"	68	1.1×10^{-4}	"	Popping based on motion picture & O-graph recording
	O	.076	66	42.4	3.22								
354	F	.064	49	50.5	3.23	45.8	1.19	1.02	"	50	1.1×10^{-4}	"	"
	O	.076	50	41.9	3.18								
355	F	.064	47	50.5	3.23	46.9	1.23	0.93	"	47	1.06×10^{-4}	175	No popping was observed
	O	.079	46.5	44.0	3.48								
356	F	.064	49	50.5	3.23	43.3	1.03	1.35	"	50	1.15×10^{-4}	165	Popping based on motion Picture & O-graph recording
	O	.066	50	36.3	2.40								
357	F	.062	51	48.9	3.03	44.8	1.21	0.97	"	51	1.11×10^{-4}	"	"
	O	.075	50	41.4	3.11								
358	F	.064	51	50.5	3.23	45.8	1.19	1.02	"	51	1.96×10^{-3}	"	"
	O	.076	50	41.9	3.18								
359	F	.064	47	50.5	3.23	45.8	1.19	1.02	"	48	1.96×10^{-3}	"	"
	O	.076	48	41.9	3.18								
360	F	.076	52.5	60.4	4.59	48.3	.079	1.02	"	54	1.03×10^{-4}	"	"
	O	.060	56.5	33.0	1.98								

Test No.		W	T	V	M	$\bar{V}_a$	O/F	M_f/M_o	D	$\bar{T}_a$	$D/\bar{V}_a$	P	Comments
361	F	.064	54.5	50.7	3.24	46.2	1.02	1.19	.060	55	1.08×10^{-4}	165	*Popping based on motion* picture & O-graph recording
	O	.065	55	41.9	2.72								
362	F	.065	52.5	51.6	3.35	45.6	1.12	1.14	"	54	1.09×10^{-4}	105	"
	O	.073	55	40.3	2.94								
363	F	.064	52.5	50.5	3.23	46.6	1.23	0.93	"	52	1.07×10^{-4}	"	"
	O	.079	53	44.0	3.48								
364	F	.065	62.5	51.6	3.35	47.5	1.23	0.95	"	61	1.05×10^{-4}	"	"
	O	.080	59.5	44.2	3.54								
365	F	.064	62.5	50.5	3.23	46.5	1.22	0.96	"	61	1.07×10^{-4}	"	"
	O	.078	59.5	43.3	3.38								
366	F	.065	62.5	51.6	3.35	47.9	1.25	0.92	"	61	1.0×10^{-4}	"	"
	O	.081	59.5	44.9	3.64								
367	F	.065	79.5	51.6	3.35	47.7	1.25	0.93	"	77	1.04×10^{-4}	"	"
	O	.081	76.0	44.7	3.62								
368	F	.062	70	49.1	3.04	46.5	1.29	0.85	"	69	1.07×10^{-4}	165	"
	O	.080	67.5	44.5	3.56								
369	F	.063	69.0	49.8	3.14	46.2	1.24	0.93	"	67	1.08×10^{-4}	"	Popping based on O-graph recording
	O	.078	69.5	43.3	3.38								
370	F	.062	64.0	49.1	3.04	44.8	1.21	0.98	"	64	1.12×10^{-4}	"	"
	O	.075	64.5	41.4	3.10								
371	F	.063	62.5	49.4	3.11	43.1	1.06	1.23	"	63	1.16×10^{-4}	"	"
	O	.067	62.5	37.2	2.49								
372	F	.062	54.5	48.6	3.01	41.3	0.98	1.45	"	55	1.21×10^{-4}	"	"
	O	.061	54.5	34.0	2.07								
373	F	.062	64	59.8	3.71	53.0	1.23	1.03	.055	63	8.64×10^{-5}	95	Popping based on motion picture & O-graph recording
	O	.076	62.5	52.1	3.60								
374	F	.062	64	59.8	3.71	54.8	1.19	0.99	.055	63	8.36×10^{-5}	95	Popping based on motion picture & O'graph recording
	O	.074	62.5	50.6	3.74								
375	F	.062	64	59.8	3.71	57.7	1.27	0.79	"	63	7.94×10^{-5}	"	"
	O	.079	62.5	54.2	4.72								
376	F	.062	64.0	59.8	3.71	56.8	1.29	0.85	"	63	8.06×10^{-5}	165	"
	O	.080	62.5	54.4	4.35								
377	F	.062	81.5	60.1	3.73	56.5	1.27	0.88	"	72	8.1×10^{-5}	175	"
	O	.079	64.5	53.6	4.23								
378	F	.062	89	60.5	3.75	57.7	1.31	0.83	"	77	7.9×10^{-5}	"	"
	O	.081	68	55.5	4.50								
379	F	.062	81.5	60.5	3.75	57.3	1.29	0.86	"	94	7.99×10^{-5}	"	"
	O	.080	104	54.7	4.38								
380	F	.063	105	60.9	3.84	56.7	1.24	0.93	"	110	8.0×10^{-5}	"	"
	O	.078	114	53.2	4.15								
381	F	.063	107	60.9	3.84	57.3	1.27	0.88	"	111	7.99×10^{-5}	"	"
	O	.080	114	54.4	4.35								
382	F	.063	110	60.9	3.85	53.2	1.21	1.08	"	111	8.6×10^{-5}	"	"
	O	.076	111	52.1	3.56								
383	F	.062	66	60.1	3.73	57.7	1.32	0.81	"	65	7.94×10^{-5}	"	"
	O	.082	65	55.9	4.58								
384	F	.062	77.5	60.4	3.74	52.9	1.29	0.99	"	83	8.66×10^{-5}	"	"
	O	.080	87.5	54.7	3.78								
385	F	.062	77.5	60.4	3.74	56.2	1.26	0.91	"	77	8.15×10^{-5}	"	"
	O	.078	76	52.9	4.13								

Test No.		W	T	V	M	$\bar{V}_a$	O/F	M_f/M_o	D	$\bar{T}_a$	$D/\bar{V}_a$	P	Comments
388	F	.058	51.0	45.9	2.66	43.5	1.29	.848	.055	49	5.1×10^{-5}	175	Popping based on O-graph recording
	O	.075	47.5	41.8	3.14								
389	F	.088	51.0	45.9	2.66	40.88	1.13	1.10	"	62	5.5×10^{-5}	175	"
	O	.066	47.5	36.5	2.41								
390	F	.058	51.0	45.9	2.66	51.65	1.71	.484	"	49	4.3×10^{-5}	175	"
	O	.099	47.5	55.2	5.50								
391	F	.075	51.5	59.7	4.51	53.9	1.17	1.04	"	49	4.1×10^{-5}	195	"
	O	.089	47.5	49.1	4.34								
392	F	.076	51.5	59.7	4.51	53.8	1.16	1.06	"	49	4.2×10^{-5}	195	"
	O	.088	47.5	48.6	4.26								
393	F	.075	60.0	59.1	4.42	48.5	.891	1.84	"	59	4.6×10^{-5}	415	Separated flow based on motion recording
	O	.066	54.5	36.5	2.40								
394	F	.090	62	71.0	6.37	65.1	1.21	.967	.060	59	7.67×10^{-5}	235	Mixed flow
	O	.109	56	60.5	6.59								
395	F	.090	52.5	70.7	6.33	60.6	1.02	1.37	"	49	8.25×10^{-5}	225	Mixed flow
	O	.091	45	50.7	4.63								
396	F	.090	45	71.1	6.4	65.0	1.20	.991	"	46	7.69×10^{-5}	235	"
	O	.108	37.5	59.8	6.5								
397	F	.090	62	71.1	6.4	66.0	1.19	1.52	"	76	7.57×10^{-5}	225	"
	O	.107	62.5	59.4	4.22								
398	F	.090	70	71.0	6.37	62.6	1.35	.931	"	71	7.98×10^{-5}	235	"
	O	.121	71	56.3	6.84								
399	F	.090	75.5	71.0	6.33	62.1	1.09	1.19	"	77	8.04×10^{-5}	235	"
	O	.099	78.5	54.2	5.30								
400	F	.090	84	71.1	6.41	61.8	1.06	1.24	.060	81	8.0×10^{-5}	235	Mixed flow
	O	.096	77.5	53.0	5.07								
401	F	.090	87	71.1	6.41	61.0	1.02	1.36	"	85	8.19×10^{-5}	235	"
	O	.092	82.5	51.2	4.72								
402	F	.087	98.5	68.8	6.24	61.1	1.60	1.32	"	90	8.18×10^{-5}	235	"
	O	.092	82.5	51.2	4.72								
403	F	.077	103	61.0	4.72	54.7	1.16	1.05	"	100	9.13×10^{-5}	255	"
	O	.089	97.5	49.8	4.48								
404	F	.076	108	50.3	3.85	49.8	1.16	.882	"	102	1.0×10^{-4}	215	"
	O	.089	96.5	49.1	4.35								
405	F	.087	112.	68.8	5.93	58.4	.993	1.44	"	106	9.9×10^{-5}	235	"
	O	.087	99	48.0	4.19								
406	F	.083	66	66.1	5.49	60.6	1.02	.98	"	64	8.24×10^{-5}	"	"
	O	.100	62.5	56.0	5.60								
407	F	.083	66	65.4	5.42	58.5	1.14	1.09	"	64	8.54×10^{-5}	"	"
	O	.094	62.5	52.4	4.94								
408	F	.088	66	65.4	5.74	61.2	1.11	1.08	"	66	8.17×10^{-5}	"	"
	O	.098	62.5	54.2	5.30								
409	F	.083	66	65.4	5.42	57.3	1.09	1.21	"	64	8.73×10^{-5}	"	"
	O	.089	62.5	49.8	4.48								
410	F	.069	85	54.3	3.74	45.4	.946	1.62	"	81	1.10×10^{-4}	185	Popping based on O-graph & motion picture recording
	O	.065	76	36.1	2.35								
411	F	.069	94.5	55.1	3.85	45.2	.877	1.85	"	92	1.11×10^{-4}	175	"
	O	.061	89	33.9	2.08								
412	F	.069	97	55.1	3.85	45.7	.919	1.69	"	92	1.09×10^{-4}	190	"
	O	.064	86.5	35.6	2.28								
413	F	.070	89	55.1	3.85	47.3	1.03	1.34	.060	85.5	1.06×10^{-4}	90	Popping based on O-graph
	O	.072	82.5	39.9	2.87								
414	F	.069	105	54.3	3.74	46.6	1.01	1.39	"	100	1.07×10^{-4}	80	Popping based on motion picture and O-graph
	O	.070	94	38.6	2.70								
415	F	.069	108	54.3	3.74	48.7	1.14	1.09	"	103	1.03×10^{-4}	85	Popping based on motion picture and O-graph
	O	.079	98	43.6	3.43								
416	F	.068	110	53.5	3.62	47.9	1.13	1.11	"	105	1.04×10^{-4}	80	Popping based on motion picture and O-graph
	O	.077	101	42.6	3.27								
417	F	.069	116	55.1	3.85	47.8	1.05	1.13	"	113	1.04×10^{-4}	80	Popping based on motion picture and O-graph
	O	.073	109	40.7	2.98								
418	F	.069	116	55.1	3.85	47.1	.95	1.43	"	109	1.06×10^{-4}	80	Popping based on motion picture and O-graph
	O	.069	102	38.6	2.69								
419	F	.068	116	54.3	3.74	45.8	.98	1.49	"	109	1.09×10^{-4}	80	Popping based on motion picture and O-graph
	O	.067	102	37.2	2.49								
420	F	.068	116	54.3	3.74	45.1	.91	1.70	"	105	1.11×10^{-4}		Popping based on motion picture, Pc not available
	O	.063	101	34.9	2.19								
421	F	.068	116	54.3	3.74	44.6	.87	1.90	"	117	1.12×10^{-4}		Popping based on motion picture, Pc not available
	O	.059	118	33.0	1.97								
422	F	.069	116	54.3	3.74	64.1	.83	2.04	"	111	1.13×10^{-4}		Popping based on motion picture, Pc not available
	O	.057	109	31.8	1.83								
423	F	.069	112	54.3	3.74	52.8	1.35	.78	"	110	9.46×10^{-5}	105	Popping based on motion picture and O-graph
	O	.093	109	51.7	4.82								
424	F	.069	114	54.3	3.74	52.2	1.32	.82	"	107.8	1.10×10^{-4}	95	Popping based on motion picture and O-graph
	O	.091	103	50.3	4.56								
425	F	.068	89	53.5	3.62	45.4	.99	1.45	"	82	1.11×10^{-4}	95	Popping based on motion picture and O-graph
	O	.067	75	37.2	2.49								
426	F	.066	81.5	53.5	3.62	44.9	.97	1.15	.060	73.1	1.10×10^{-4}	95	Popping based on O-graphs
	O	.066	64.5	36.2	2.39								
427	F	.069	81.5	54.7	3.76	45.3	.91	1.72	"	80.4	1.10×10^{-4}	"	Popping based on O-graphs
	O	.063	9	34.9	2.20								
428	F	.069	108	54.7	3.78	47.1	1.04	1.33	"	106	1.06×10^{-4}	"	Popping based on O-graphs
	O	.072	104	39.7	2.85								
429	F	.069	114	54.7	3.78	45.7	.95	1.59	"	110	1.09×10^{-4}	"	Popping based on O-graph and motion pictures.
	O	.066	106	36.3	2.38								
430	F	.060	75	58.2	3.48	53	1.19	1.0	.055	71.	8.64×10^{-5}	185	Popping based on O-graph and motion picture
	O	.071	68	48.7	3.48								
431	F	.060	93	58.5	3.52	52.2	1.14	1.1	"	86.4	8.78×10^{-5}	175	Popping based on O-graph and motion pictures
	O	.069	81	46.7	3.20								
432	F	.076	101	74.0	5.64	69.4	1.26	.89	"	96	6.60×10^{-5}	215	No popping. (Mixed)
	O	.096	92.5	65.4	6.34								
433	F	.076	106	73.5	5.55	68.4	1.23	.91	"	101	6.69×10^{-5}	"	No Popping (Mixed)
	O	.094	97.5	64.4	6.08								
434	F	.062	114	64.5	4.00	57.0	1.20	1.06	"	107	8.03×10^{-5}	175	No popping (Mixed)
	O	.075	101	51.0	3.79								
435	F	.062	106	60.4	3.75	54.8	1.18	1.02	"	101	8.36×10^{-5}	75	Popping based on O'graph recording
	O	.073	96	50.1	3.68								
436	F	.062	96.5	59.8	3.68	52.3	1.08	1.23	"	79	4.3×10^{-5}	95	Popping based on O-graph recording
	O	.066	72.5	45.2	3.0								
437	F	.062	77.5	59.8	3.68	52.3	1.08	1.23	"	73	4.3×10^{-5}	"	Popping based on O-graph recording
	O	.066	68.0	45.2	3.0								
438	F	.028	105	50.8	1.41	52.8	1.52	.62	.040	101	6.3×10^{-5}	45	Mixed flow
	O	.042	99	54.1	2.27								
439	F	.029	112	53.4	1.55	51.3	1.32	.81	.040	102	6.5×10^{-5}	45	Mixed flow
	O	.038	94	49.5	1.91								

Test No.		W	T	V	M	$\bar{V}_a$	O/F	M_f/M_o	D	$\bar{T}_a$	$D/\bar{V}_a$	P	Comments
440	F	.033	102	58.[illegible]	1.[illegible]4	[illegible]8.3	1.3	.7[illegible]6	"	80	[illegible]x10[illegible]	"	Mixed flow
	O	.045	97.[illegible]	5[illegible].4	2.35								
441	F	.030	97	53.4	1.[illegible]5	50.8	1.[illegible]0	.84	"	95	6.5×10^{-5}	"	Mixed flow
	O	.038	91	48.8	1.84								
442	F	.029	116	53.4	1.55	56.5	1.[illegible]	.58	"	111	5.9×10^{-5}	"	Mixed flow
	O	.045	107	58.5	2.05								
443	F	.029	125	53.4	1.55	53.8	1.45	.68	"	118	6.2×10^{-5}	"	Separated flow due to OX boiling.
	O	.042	114	54.12	2.27								
444	F	.029	108	53.4	1.55	57.4	1.60	.55	"	108	5.8×10^{-5}	"	Mixed flow
	O	.047	108	60.	2.98								
445	F	.031	122	57.4	1.80	53.3	1.24	.93	"	117	6.2×10^{-5}	"	Separated flow due to OX boiling
	O	.039	114	50.0	1.94								
446	F	.031	126	57.4	1.79	52.9	1.24	.96	"	121	6.29×10^{-5}	"	Separated flow due to OX boiling
	O	.038	116	49.3	1.86								
447	F	.036	122	66.6	2.42	58.3	1.08	1.22	"	114	5.7×10^{-5}	"	Mixed flow
	O	.039	108	50.6	1.98								
448	F	.036	114	66.6	2.42	59.9	1.16	1.06	"	110	5.56×10^{-5}	55	Mixed flow
	O	.042	104	54.1	2.27								
449	F	.036	116	66.7	2.42	59.9	1.16	1.06	"	110	5.55×10^{-5}	"	Mixed flow
	O	.042	106	57.2	2.28								
450	F	.036	118	66.6	2.47	59.9	1.16	1.06	"	110	5.56×10^{-5}	"	Mixed flow
	O	.042	104	54.2	2.27								
451	F	.037	106	68.2	2.53	57.2	1.13	2.57	"	103	5.8×10^{-5}	45	Mixed flow
	O	.035	101	45.7	1.62								
452	F	.035	108	65.1	2.3	54.8	.97	1.51	.040	103	6.08×10^{-5}	45	Mixed flow
	O	.034	97.5	44.4	1.53								
453	F	.035	105	65.1	2.30	55.1	.98	1.47	"	98	6.05×10^{-5}	50	Mixed flow
	O	.035	91	44.9	1.56								
454	F	.039	132	40.9	2.74	60.4	1.0	1.43	"	123	5.52×10^{-5}	65	Mixed flow
	O	.039	114	49.8	1.92								
455	F	.037	134	68.2	2.53	67.9	1.41	.712	"	127	4.9×10^{-5}	50	Separated flow due to OX boiling
	O	.053	122	67.7	3.55								
456	F	.036	137	66.6	2.42	62.1	1.25	.913	"	133	5.36×10^{-5}	55	Separated flow due to OX boiling
	O	.045	129	58.5	2.65								
457	F	.036	144	66.3	2.42	63.1	1.29	.852	"	139	5.27×10^{-5}	"	Separated flow due to OX boiling
	O	.047	135	60.5	2.84								
458	F	.035	144	64.1	2.24	61.7	1.33	.801	"	137	5.4×10^{-5}	"	Separated flow due to OX boiling
	O	.047	131	60.0	2.79								
459	F	.036	147	62.3	2.11	60.1	1.34	.797	"	142	5.55×10^{-5}	"	Separated flow due to OX boiling
	O	.045	137	58.5	2.65								
460	F	.084	64	66.3	5.56	53.6	.814	2.15	.060	63	9.3×10^{-5}	470	Separated flow based on motion picture recording
	O	.068	61.5	37.9	2.59								
461	F	.085	66.	66.9	5.68	64.7	1.34	.789	"	64	7.7×10^{-5}	565	Separated flow based on motion picture recording
	O	.114	62.5	65.1	7.19								
462	F	.087	66.	68.8	5.99	58.7	1.00	1.42	"	64	8.5×10^{-5}	535	Separated flow based on motion picture recording
	O	.067	62.5	48.4	4.23								
463	F	.087	64.	68.8	5.99	57.9	.96	1.54	"	65	8.6×10^{-5}	"	Separated flow based on motion picture recording
	O	.084	67.	46.6	3.91								
464	F	.087	69.5	68.8	5.99	62.2	1.17	1.04	"	67	8.0×10^{-5}	585	Separated flow based on motion picture recording
	O	.102	66.	56.5	5.77								
465	F	.087	64	68.8	5.99	64.6	1.26	.89	.060	66	7.7×10^{-5}	475	Separated flow based on motion picture recording
	O	.110	67	61.3	6.74								
466	F	.063	52.5	65.7	5.45	59.8	1.19	1.00	"	49	8.36×10^{-5}	435	Separated flow based on motion picture recording
	O	.099	46.5	54.9	5.43								
467	F	.063	52.5	65.7	5.45	60.27	1.21	.97	"	49	8.3×10^{-5}	455	Separated flow based on motion picture recording
	O	.101	48	55.9	5.63								
468	F	.083	110	65.7	5.45	63.5	1.35	.79	"	109	7.87×10^{-5}	"	Separated flow based on motion picture recording
	O	.112	108	61.9	6.93								
469	F	.087	116	68.8	6.0	65.3	1.25	.91	"	115	7.78×10^{-5}	"	Separated flow based on motion picture recording
	O	.109	114	60.4	6.59								
470	F	.087	119	68.8	6.0	63.1	1.21	.98	"	115	7.93×10^{-5}	445	Separated flow based on motion picture recording
	O	.105	111	58.2	6.11								
471	F	.067	92	52.8	3.53	49.3	1.26	.90	"	68	1.01×10^{-4}	100	Popping based on motion pictures & O-graph record
	O	.084	96	46.6	3.91								
472	F	.067	72	52.6	3.50	47.7	1.15	1.07	"	64	1.05×10^{-5}	"	Popping based on motion pictures & O-graph record
	O	.077	64.5	42.6	3.27								
473	F	.067	70	52.6	3.50	49.2	1.26	.90	"	66	1.02×10^{-5}	"	Popping based on motion pictures & O-graph record
	O	.084	63	46.6	3.91								
474	F	.067	62	52.6	3.50	47.3	1.16	1.06	"	61	1.05×10^{-4}	"	Popping based on motion pictures & O-graph record
	O	.077	59.5	42.8	3.3								
475	F	.042	64	77.9	3.30	68.3	1.09	1.20	.040	66	4.88×10^{-5}	630	Separated flow based on motion picture recording
	O	.046	68	59.5	2.74								
476	F	.045	64	81.7	3.64	77.09	1.28	.87	"	66	4.32×10^{-5}	80	Mixed flow based on motion picture recording
	O	.057	68	73.5	4.19								
477	F	.045	66	83.2	3.77	72	1.05	1.29	"	64	4.6×10^{-5}	85	Mixed flow based on motion picture recording
	O	.048	61	61.3	2.91								
478	F	.038	66	70.	2.67	67.4	1.33	.807	.040	62	4.94×10^{-5}	640	Mixed flow based on motion picture recording
	O	.051	59.5	65.4	3.31								
479	F	.067	71.5	52.8	3.53	49.3	1.25	.905	.060	69	1.01×10^{-4}	100	Popping based on motion pictures & O'graph record
	O	.084	68	46.5	3.90								
480	F	.068	64	53.7	3.64	50.7	1.28	.86	"	66	9.86×10^{-5}	"	Popping based on motion pictures & O-graph record
	O	.087	68	48.4	4.22								
481	F	.045	132	35.1	1.56	30.8	1.06	1.24	"	129	1.62×10^{-4}	23	Popping based on motion pictures & O-graph record
	O	.048	128	26.5	1.26								
482	F	.044	141	34.9	1.54	30.1	1.03	1.33	"	138	1.66×10^{-4}	147	Popping based on O-graph recording
	O	.046	135	25.4	1.16								
483	F	.035	60.5	65.1	2.30	54.3	.946	1.60	"	66	6.14×10^{-5}	175	N_2H_4+5%NH_4NO_3. Popping based on O-graph record
	O	.034	51.5	43.1	1.44								
484	F	.035	60.5	64.1	2.24	58.6	1.20	.986	"	56	5.68×10^{-5}	185	"
	O	.041	51.5	54.1	2.27								
485	F	.034	60.5	62.6	2.13	57.9	1.23	.938	"	59.	5.75×10^{-5}	220	N_2H_4+5%$N_2H_4NO_3$ Rough chamber pressure
	O	.042	57.5	54.1	2.27								
486	F	.017	58.5	64.1	1.07	56.9	2.51	.471	.040	55	5.86×10^{-5}	90	N_2H_4+5%NH_4NO_3 Mixed flow
	O	.042	54.5	54.1	2.27								
487	F	.034	58.5	63.1	2.16	58.1	1.22	.952	"	57	5.73×10^{-5}	100	"
	O	.042	56	54.1	2.27								
488	F	.035	58.5	63.8	2.22	58.5	1.21	.970	"	57	5.69×10^{-5}	100	"
	O	.042	56	54.1	2.27								
489	F	.035	58.5	63.8	2.22	58.5	1.21	.970	"	57	5.69×10^{-5}	100	"
	O	.042	56	54.1	2.27								
490	F	.024	62.5	43.4	1.02	41.0	1.31	.83	"	63	8.12×10^{-5}	150	"
	O	.031	62.5	39.8	1.23								
491	F	.024	56.5	43.4	1.02	40.4	1.25	.91	.040	54	8.24×10^{-5}	30	N_2H_4+5%NH_4NO_3 Mixed flow
	O	.029	51.5	38.0	1.12								

Test No.		W	T	V	M	$\bar{V}_a$	O/F	M_f/M_o	D	$\bar{T}_a$	$D/\bar{V}_a$	P	Comments
492	F	.023	60	41.4	.931	40.5	1.37	.75	"	57	[illegible]	"	"
	O	.031	54.5	[illegible]	1.23								
493	F	.022	60	40.8	.907	36.7	1.16	1.06	"	58	9.07×10^{-5}	"	N_2H_4+5%NH_4NO_3 Mixed flow
	O	.026	56	33.2	.852								
494	F	.022	62	40.8	.907	37.1	1.16	1.04	"	59	[illegible]	"	"
	O	.026	56	35.9	.871								
495	F	.024	64.5	43.4	1.02	40.5	1.26	.90	"	60	8.22×10^{-5}	35	"
	O	.029	58	36.3	1.14								
496	F	.024	66	43.4	1.02	37.8	1.21	.98	"	61	8.38×10^{-5}	"	"
	O	.029	56	36.6	1.05								
497	F	.024	66	44.8	1.09	42.1	1.27	.83	"	60	7.52×10^{-5}	30	N_2H_4+5%UDMH Mixed flow
	O	.031	56	39.6	1.23								
498	F	.024	66	44.6	1.09	42.1	1.27	.88	"	61	7.3×10^{-5}	"	"
	O	.021	58	39.8	1.23								
499	F	.024	64.5	43.4	1.02	41.4	1.31	.83	"	58	6.05×10^{-5}	"	"
	O	.031	56	39.8	1.23								
500	F	.024	66	43.4	1.02	41.4	1.31	.83	"	60	6.06×10^{-5}	"	"
	O	.031	56	39.8	1.23								
501	F	.021	74	38.3	.796	34.2	1.14	1.09	"	67	9.7×10^{-5}	"	"
	O	.024	62.5	30.6	.726								
502	F	.020	69.5	37.3	.756	34.9	1.27	.86	"	66	9.5×10^{-5}	"	"
	O	.026	64.5	33.2	.853								
503	F	.021	74	38.3	.796	35.5	1.23	.93	"	69	9.4×10^{-5}	"	"
	O	.026	66	33.2	.853								
504	F	.017	74	31.2	.526	32.7	1.54	.598	.040	69	1.02×10^{-5}	30	N_2H_4+5%UDMH Mixed flow
	O	.026	64.5	33.7	.870								
505	F	.009	92	17.23	.162	19.47	1.71	.488	.040	82	1.71×10^{-4}	14.7	N_2H_4+5%UDMH-Separated flow due to OX boiling
	O	.016	72	20.68	.331								
506	F	.012	72	21.7	.256	21.52	1.4	.721	.040	72	1.55×10^{-4}	"	"
	O	.017	72	21.4	.355								
507	F	.007	71	27.41	.186	37.42	2.2	.296	.027	71	6.03×10^{-5}	"	N_2H_4+5% MMH, Separated flow due to OX boiling
	O	.015	71	41.37	.629								
508	F	.010	70	39.2	.380	39.9	1.48	.65	.027	69	5.6×10^{-5}	"	N_2H_4+5% MMH Mixed flow
	O	.014	68	40.34	.581								
509	F	.013	68	53.23	.703	49.8	1.27	.89	.027	66	4.5×10^{-5}	"	"
	O	.017	68	47.07	.791								